© 2022. Published by The Company of Biologists Ltd | Journal of Cell Science (2022) 135, jcs259120. doi:10.1242/jcs.259120

RESEARCH ARTICLE

PLK1 controls centriole distal appendage formation and centrobin removal via independent pathways

Morgan Le Roux-Bourdieu[1,*,‡,§], Devashish Dwivedi[1,‡], Daniela Harry[1] and Patrick Meraldi[1,2,§]

ABSTRACT

Centrioles are central structural elements of centrosomes and cilia. In human cells, daughter centrioles are assembled adjacent to existing centrioles in S-phase and reach their full functionality with the formation of distal and subdistal appendages one-and-a-half cell cycles later, as they exit their second mitosis. Current models postulate that the centriolar protein centrobin acts as placeholder for distal appendage proteins that must be removed to complete distal appendage formation. Here, we investigated, in non-transformed human epithelial RPE1 cells, the mechanisms controlling centrobin removal and its effect on distal appendage formation. Our data are consistent with a speculative model in which centrobin is removed from older centrioles due to a higher affinity for the newly born daughter centrioles, under the control of the centrosomal kinase PLK1. This removal also depends on the presence of subdistal appendage proteins on the oldest centriole. Removing centrobin, however, is not required for the recruitment of distal appendage proteins, even though this process is equally dependent on PLK1. We conclude that PLK1 kinase regulates centrobin removal and distal appendage formation during centriole maturation via separate pathways.

KEY WORDS: Centrosome, Polo-like-kinase 1, Centrobin, Cell cycle, Mitosis

INTRODUCTION

Centrosomes are the main microtubule nucleating and organizing centres of metazoan cells. Each centrosome is composed of two barrel-shaped centrioles, composed of nine microtubule triplets surrounded by pericentriolar material (PCM) (Gönczy and Hatzopoulos, 2019; Vásquez-Limeta and Loncarek, 2021). Like DNA, centrosomes replicate in a semi-conservative manner once per cell cycle. In G1, human somatic cells contain two centrioles that have become dis-engaged – one older centriole, called here the 'grandmother' centriole, and one younger daughter centriole. As both centrioles give rise orthogonally to one 'daughter' centriole during S-phase, the G1 daughter centriole becomes the 'mother' centriole. The two new-born daughter centrioles elongate in G2, followed by centrosome separation and maturation at mitotic onset. Therefore, mitotic cells always contain three different centriole generations – one grandmother centriole, one mother centriole and two daughter centrioles.

One key difference between the grandmother centriole and the mother centriole is the presence of distal and subdistal appendages on the grandmother centriole that emerge as spikes from the centriolar barrel (Tischer et al., 2021). The transition from nascent daughter centriole to grandmother centriole via mother centriole encompasses two mitoses, and one and a half cell cycles (Kong et al., 2014). During the second mitosis, the mother centriole gradually recruits the full set of distal and subdistal appendage proteins, driving the formation of both appendages in the next G1 to complete the transformation into a grandmother centriole. Each type of appendage ensures key centrosomal or ciliary functions (Loncarek and Bettencourt-Dias, 2018). Subdistal appendages enable centrioles to anchor and focus microtubules directing intracellular trafficking, cell motility, cell adhesion or cell polarity during interphase (Bornens, 2002; Delgehyr et al., 2005). At its core, sitting on the centriole wall, resides cenexin (also known as ODF2), which is required for the recruitment of all the proteins that are located in the outer parts of subdistal appendages, such as CEP128, centriolin and ninein (Chong et al., 2020; Mazo et al., 2016). Distal appendages are required for the hook-like insertion of the older centriole into the plasma membrane during ciliogenesis (Tanos et al., 2013). The binding of OFD1 is the first building step for the formation of distal appendages (Wang et al., 2018). This protein plays a pleiotropic role regulating distal appendage formation, centriole length and ciliogenesis (Singla et al., 2010). In terms of distal appendage formation, OFD1 binding enables the hierarchical recruitment of all subsequent proteins at mother centrioles, starting with CEP83 and ending with FBF1 and CEP164 (Wang et al., 2018). Super-resolution microscopy further revealed that distal and subdistal appendages proteins mutually influence each other's position relative to the centriole, indicating that they are structurally partially inter-dependent (Chong et al., 2020).

A central player in the current regulatory model of distal appendage formation is centrobin. This protein accumulates in human epithelial cells on daughter centrioles (Zou et al., 2005); it is required for efficient centriole elongation during centrosome duplication and essential for cilia formation (Gudi et al., 2014; Ogungbenro et al., 2018). In the context of distal appendage formation, centrobin has been proposed to act as a placeholder for the recruitment of future distal appendage proteins, and its removal in human epithelial cells under the control of the centriole protein Talpid3 (also known as KIAA0586) is thought to allow the recruitment of OFD1 (Wang et al., 2018). This raises the question as to the exact timing of centrobin removal during the centrosome cycle, and the nature of the regulatory pathways controlling this process. The organism in which centrobin has been best studied is *Drosophila melanogaster*, where its functions and exact localization

[1]Department of Cell Physiology and Metabolism, Faculty of Medicine, University of Geneva, 1211 Geneva, Switzerland. [2]Translational Research Centre in Onco-haematology, Faculty of Medicine, University of Geneva, 1211 Geneva, Switzerland.
*Present address: AC Immune SA, EPFL Innovation Park, 1015 Lausanne, Switzerland.
‡These authors contributed equally to this work

§Authors for correspondence (Patrick.Meraldi@unige.ch; morgan.le-roux-bourdieu@acimmune.com)

P.M., 0000-0001-9742-8756

Handling Editor: David Glover
Received 11 July 2021; Accepted 18 March 2022

Journal of Cell Science

Journal of Cell Science (2022) 135, jcs259120. doi:10.1242/jcs.259120

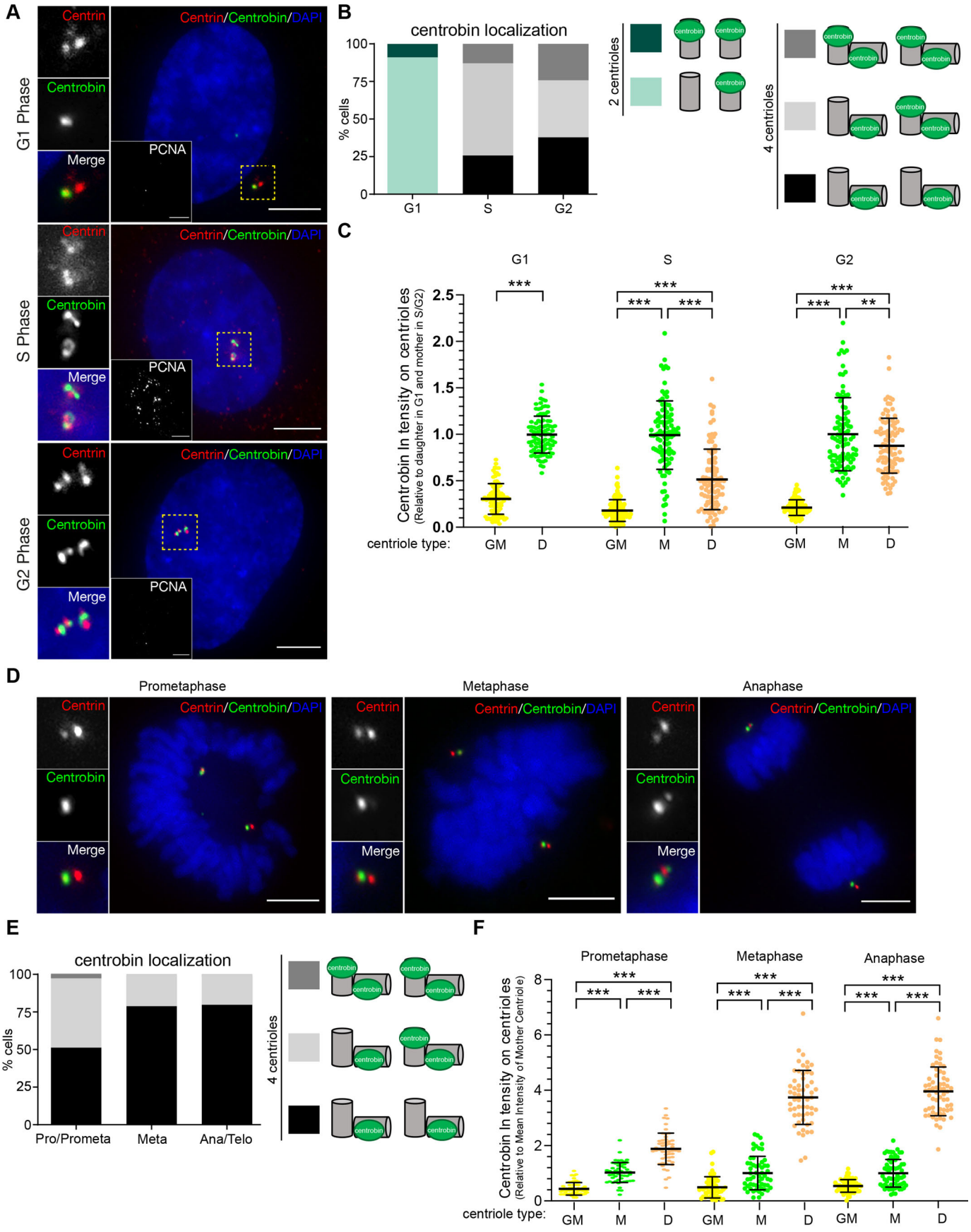

Fig. 1. See next page for legend.

Journal of Cell Science

Journal of Cell Science (2022) 135, jcs259120. doi:10.1242/jcs.259120

Fig. 1. Centrobin is removed from mother centrioles at the prometaphase/metaphase transition. (A) Immunofluorescence images of hTert-RPE1-eGFP-centrin1 cells stained with DAPI and antibodies against centrobin and PCNA. (B) Quantification of the centrobin localization pattern in hTert-RPE1-eGFP-centrin1 cells in G1 (*N*=3 independent experiments, *n*=133 cells), S (*N*=3, *n*=31 cells) or G2 (*N*=3, *n*=74 cells) based on the PCNA signal. (C) Quantification of the relative centrobin intensity on individual grandmother (GM), mother (labeled M) and daughter centrioles (labeled D). Values were normalized to the average mother centriole intensity in S (*N*=3, *n*=98 cells) and G2 (*N*=3, *n*=95 cells), to the daughter centriole intensity in G1 (*N*=3, *n*=99 cells); ***P*<0.01, ****P*<0.001 (one-way ANOVA with Sidak's multiple comparison test). Error bars indicate s.e.m. (D) Immunofluorescence images of hTert-RPE1-eGFP-centrin1 cells stained with antibodies against centrobin and DAPI. (E) Quantification of the centrobin localization pattern in hTert-RPE1-eGFP-centrin1 cells in prophase and prometaphase (Pro/Prometa; *N*=2, *n*=63 cells), metaphase (Meta; *N*=2, *n*=85 cells) and anaphase and telophase (*N*=2, *n*=74 cells). (F) Quantification of the relative centrobin intensity on individual grandmother (GM), mother (M) and daughter centrioles (D) during prometaphase (*N*=3, *n*=54 cells), metaphase (*N*=3, *n*=57 cells) and anaphase (Ana/Telo; *N*=3, *n*=63 cells). Values were normalized to the average mother centriole intensity. ****P*<0.001 (one-way ANOVA with Sidak's multiple comparison test). Error bars indicate s.e.m. Scale barss: 5 µm.

can vary from cell type to cell type. Centrobin inhibits basal body function in sensory neurons, but promotes basal body elongation in spermatocytes (Gottardo et al., 2015; Reina et al., 2018); likewise centrobin promotes the recruitment of interphase pericentriolar material in neuroblasts but not in epithelial wing cells (Januschke et al., 2013). The best-studied regulator of centrobin in flies is the polo-like kinase 1 (PLK1). In interphase *Drosophila* neuroblast, centrobin is exclusively present on the younger centrosome containing the daughter centriole; as this daughter centriole becomes itself a mother centriole, centrobin is removed in a PLK1-dependent manner during mitosis (Gallaud et al., 2020; Januschke et al., 2013, 2011). In human epithelial cells, PLK1 can phosphorylate centrobin in mitosis (Lee et al., 2010). Moreover, PLK1 kinase activity regulates directly or indirectly the levels of several distal appendage components throughout the cell cycle: its activity is required for the reduction of CEP164 on the grandmother centriole as cells reach prophase, but it is also required for the appearance of CEP164 on the mother centriole, which starts as cells progress through mitosis (Kong et al., 2014). Therefore, it is thought that PLK1 promotes the formation of distal appendages including the recruitment of CEP164 via the removal of centrobin from the mother centriole. This hypothesis has, however, never been tested in one coherent model system or cell line, which is important given the cell type-to-cell type variability in centrobin function. Here, we tested the localization pattern of centrobin over the cell cycle, its potential regulation by PLK1, and its role in the recruitment of distal appendage protein recruitment, in non-malignant diploid human retina pigment epithelial RPE1 cells as this cell line has been used to propose the placeholder model (Wang et al., 2018). Furthermore, we tested how subdistal appendage proteins contribute to centrobin dynamics, as the subdistal appendage protein cenexin is a key regulator of PLK1 activity (Colicino et al., 2019). We show that centrobin is removed from the mother centriole as cells reach metaphase, and that this removal depends on the newly emerging daughter centrioles, possibly because of higher affinity binding sites. Centrobin removal and recruitment of distal appendage proteins depend both on PLK1 activity and the presence of cenexin. Surprisingly, these two centrosome cycle steps occur independently of each other. Indeed, in multiple siRNA or CRISPR/Cas9 knockout backgrounds, distal appendage protein recruitment occurs in RPE1 cells without centrobin removal. We propose that in RPE1 cells PLK1 and subdistal appendage proteins regulate the removal of centrobin and the build-up of distal appendages via separate pathways, pointing for a need to revise the regulatory model for centriole maturation.

RESULTS

Centrobin is removed from the mother centriole at the prometaphase-metaphase transition

Centrobin was first described as a daughter centriole-specific protein that localizes to the daughter centriole in G1 before appearing on the two new daughter 'pro'-centrioles that arise from the grandmother and the new 'mother' centriole in S-phase (Zou et al., 2005). How and when centrobin is removed from the mother centriole in human cells is, however, unknown. To address the when, we studied the cell cycle-dependent localization of centrobin in human retina-pigment epithelial cells immortalized with telomerase and expressing the centriole marker eGFP–centrin1 (hTertRPE1-eGFP-centrin1). Cells were fixed for immunofluorescence, stained for centrobin, the S-phase marker PCNA and the DNA marker DAPI, and assigned to: (1) G1, if the cell was PCNA-negative and contained two centrioles; (2) S-phase, if the cell was PCNA-positive (note that only cells with four distinct centrioles were considered); or (3) G2, if the cell was PCNA-negative and contained four centrioles. In addition, an increasing abundance of eGFP–centrin1 on daughter, mother and grandmother centrioles allowed the classification of each centriole in one of those age categories (Tan et al., 2015). Centrobin localization on the different type of centrioles was assessed both in a qualitative manner (present or not present), as well as in a quantitative manner (mean intensity per centriole type) to reveal the full spectrum of localizations. In most G1 cells, centrobin was only visibly present on the daughter centriole (91±4%; mean±s.e.m.), with mean intensity that was at least 3 times higher than on the grandmother centriole (Fig. 1A–C). In S-phase cells that had initiated centriole duplication (with the daughter centriole becoming a mother), and hence contained four eGFP–centrin1 dots, most cells displayed centrobin on both daughter centrioles and the mother centriole (64.5±7%; Fig. 1A,B). The signal on mother centrioles was roughly two times brighter than on the daughter centrioles (Fig. 1C). Finally, in G2 we observed a mix of three populations: 27.4±5.6% cells with centrobin on all four centrioles, 34.3±4.7% of cells with centrobin on the mother and the two daughter centrioles, and 38.2±3.7% of cells with centrobin only on the two daughter centrioles (Fig. 1A,B; the apparent increase in the percentage of centrobin-positive grandmother centrioles was not statistically significant). The signal intensity on daughter and mother centrioles was roughly equivalent. We conclude that centrobin localization is more dynamic than previously estimated, that centrobin is gradually recruited to daughter centrioles and that centrobin can simultaneously be present on daughter and mother centrioles or even the grandmother centriole up to G2 phase.

To determine the exact time-point at which centrobin is removed from mother centrioles, we next analyzed its localization pattern in the different mitotic phases, using DAPI to determine the mitotic stage. In prophase and prometaphase, roughly half the cells still displayed centrobin on the daughter centrioles and the mother centriole, while the other half contained only two centrobin dots on the daughter centrioles; centrobin levels on daughter centrioles were on average twice as high as on mother centrioles (Fig. 1D–F). From metaphase on, 79% of the cells only displayed two centrobin dots on the daughter centrioles, with average levels that were four times higher than mother centrioles; these values did not significantly change once cells reached anaphase and telophase (Fig. 1D–F).

Journal of Cell Science (2022) 135, jcs259120. doi:10.1242/jcs.259120

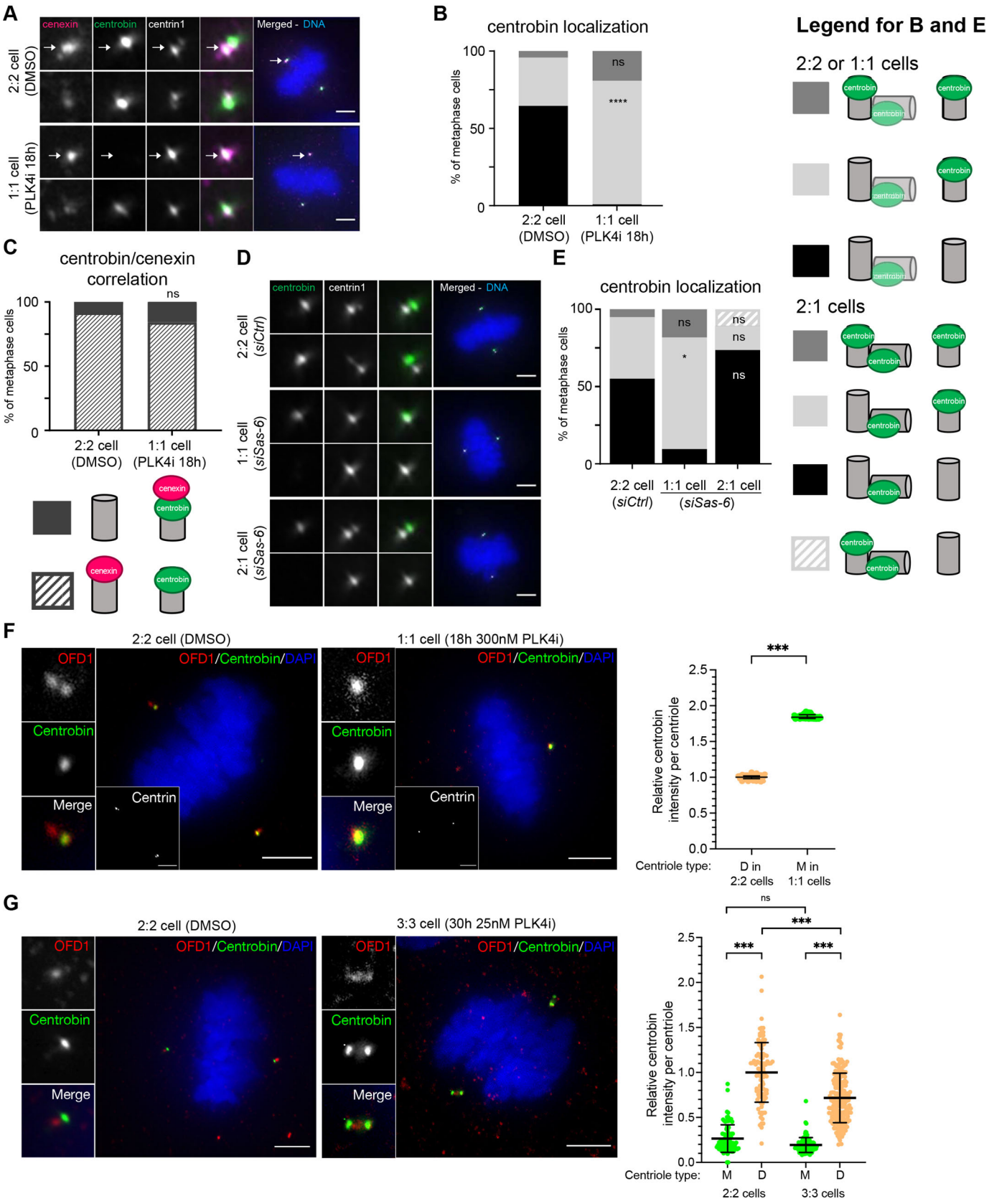

Fig. 2. See next page for legend.

Journal of Cell Science (2022) 135, jcs259120. doi:10.1242/jcs.259120

Fig. 2. Daughter centrioles compete for centrobin binding with mother centrioles. (A) Immunofluorescence images of metaphase hTert-RPE-eGFP-centrin1 cells stained with DAPI and antibodies against cenexin and centrobin after DMSO treatment or PLK4 inhibition for 18 h. White arrows identify the older centrosome. (B) Quantification of the centrobin localization pattern in hTert-RPE1-eGFP-centrin1 cells treated with DMSO (*N*=5 independent experiments, *n*=151 cells) or centrinone (*N*=5, *n*=182 cells) for 18 h. ****$P<0.0001$ (two-way ANOVA with Tukey's multiple comparison test). (C) Quantification of the centrobin and cenexin colocalization in hTertRPE1-1-eGFP-CENP-A/centrin1 cells after DMSO-treatment (*N*=4, *n*=26 cells) or PLK4 inhibition (*N*=4, *n*=75 cells) for 18 h. (D) Immunofluorescence images of metaphase hTertRPE1 eGFP-centrin1 cells treated with *siCtrl* or *siSas-6* for 24 h and stained with DAPI and centrobin antibodies. (E) Quantification of the centrobin localization pattern in hTert-RPE1-eGFP-centrin1 cells after control (*N*=3, *n*=152 cells) or Sas-6 (*N*=3, *n*=104 cells) depletion. *$P<0.05$ (two-way ANOVA with Tukey's multiple comparison test). (F) Immunofluorescence images of hTert-RPE1-eGFP-centrin1 cells stained for OFD1 (a marker for grandmother/mother centrioles) and centrobin, and treated with DMSO or with 18 h 250 nM PLK4 inhibitor to obtain 1:1 cells (left). Right panel shows the quantification of the centrobin levels per centriole in daughter centrioles of 2:2 cells (*N*=3, *n*=100 cells) versus mother centrioles of 1:1 cells (*N*=3, *n*=100 cells). ***$P<0.001$ (unpaired two-tailed *t*-test). Error bars indicate s.e.m. (G) Immunofluorescence images of hTert-RPE1-eGFP-centrin1 cells stained for OFD1 and centrobin and treated with DMSO or with 25 nM PLK4 inhibitor for 30 h to obtain 3:3 cells (left). Right panel shows the quantification of the centrobin levels per centriole in mother and daughter centrioles of 2:2 (*N*=3, *n*=86 cells) and 3:3 (*N*=3, *n*=103 cells) cells. ***$P<0.001$; ns, not significant (one-way ANOVA with Sidak's multiple comparison test). Error bars indicate s.e.m. Scale bars: 5 µm.

Staining with a second, independent, centrobin antibody led to equivalent results (Fig. S1). We conclude that centrobin is gradually removed from the mother centriole to accumulate on daughter centrioles, and that the last step in this process occurs at the prometaphase/metaphase transition.

Centrobin is removed from mother centriole possibly due to a higher affinity for daughter centrioles

To better understand the pathways controlling centrobin localization, we next tested whether centrobin removal was linked to the formation of fully elongated daughter centrioles in mitosis. To eliminate daughter centrioles, we inhibited the master regulator of centriole duplication PLK4, with the chemical inhibitor centrinone for 18 h (Wong et al., 2015). This resulted in cells that entered mitosis with only one centriole at each centrosome (called '1:1' cells). When compared to DMSO-treated '2:2' cells or to 2:2 cells that were only treated for 2 h with centrinone, 1:1 cells formed structurally normal spindle poles in mitosis as measured by the recruitment of γ-tubulin and pericentrin, two of the main components of the pericentriolar matrix (Fig. S2A–D). Moreover, these centrosomes were as functional as normal centrosomes with two centrioles; 1:1 cells had the same mitotic timing and the same chromosome segregation error rate when released from a prometaphase arrest induced with the centrosome separation (Eg5; also known as KIF11) inhibitor STLC (DeBonis et al., 2004) as did DMSO-treated or 2:2 cells treated with centrinone for only 2 h (Fig. S2E–H). This contrasted with RPE1 cells lacking centrioles on one (1:0 cells) or both poles (0:0 cells), which we and others have found to spend more time in mitosis and to have an elevated chromosome segregation error rate (Dudka et al., 2019; Wong et al., 2015).

When we analyzed the localization of centrobin in metaphase 1:1 cells, we found that 79.9±6.3% (mean±s.e.m.) contained a single centrobin-positive centriole (Fig. 2A,B). Using antibodies against the subdistal appendage protein cenexin (grandmother centriole marker; Lange and Gull, 1995), we established that this centriole was, as a rule, the mother centriole (Fig. 2A,C). The persistence of centrobin on the mother centriole in metaphase was not due to centrinone per se, since a short 2-h centrinone treatment in control 2:2 cells did not maintain centrobin at the mother centriole (Fig. S2I). Moreover, inhibition of centrosome duplication by depletion of the centriole duplication seed SAS-6 (also known as SASS6) for 24 h (Leidel et al., 2005), gave identical outcome to an 18-h inhibition of PLK4, confirming the specificity of our result (Fig. 2E; Fig. S2J).

The presence of centrobin on the mother centriole in metaphase 1:1 cells could be explained by two hypotheses: either centrobin removal requires the younger centriole to become a 'mother' that gave birth to a daughter centriole, or it is removed from mother centrioles due to the presence of a higher affinity site on the fully elongated daughter centrioles. To differentiate between the two possibilities, we looked at the cells depleted for SAS-6 for 24 h, which in our experience can lead to the formation of 2:1 cells, in which only the grandmother centriole gives rise to a daughter pro-centriole (Fig. S2J; Tan et al., 2015). The vast majority of 2:1 cells contained one centrobin-positive daughter centriole associated to the grandmother centriole, and no centrobin on the mother centriole (Fig. 2E). These data indicate that the mother centriole can 'lose' centrobin despite not having given rise to a daughter centriole, and are consistent with a model in which centrobin is removed from the mother centriole due to a higher affinity for this protein on daughter centrioles.

To further substantiate this hypothesis, we next compared the centrobin levels on the mother centriole of 1:1 cells, to the centrobin intensities of daughter centrioles in 2:2 cells by quantitative immunofluorescence. Our results indicated that mother centrioles in 1:1 cells contained nearly twice as much centrobin (Fig. 2F), consistent with re-distribution of the mitotic centrobin pool on both daughter centrioles in 2:2 cells. In addition, by partially inhibiting PLK4 with 25 nM centrinone, we also generated cells, in which grandmother and mother centrioles gave rise to two daughter centrioles. This counterintuitive result arises because partial inhibition most likely suffices to block the trans-phosphorylation-dependent PLK4 degradation without blocking its ability to initiate centriole biogenesis, as has been previously seen after the overexpression of catalytically inactive PLK4 (Guderian et al., 2010). Therefore, after 30 h of 25 nM centrinone treatment, we frequently observed spindle poles containing either a mother or a grandmother centriole each surrounded by two daughter centrioles (Fig. 2G). Quantification of centrobin intensities in such 3:3 cells indicated that both daughter centrioles only contained on average ∼60% of the centrobin levels seen on spindle poles with single daughter centrioles in 2:2 cells, suggesting again a re-distribution on all centrioles. Although the intensities showed a strong cell-to-cell variability, the overall pattern was again consistent with an affinity model in which centrobin is redistributed on daughter centrioles during mitosis.

Distal appendage proteins are recruited to the mother centriole independently of centrobin removal

Recent studies postulated that distal appendage formation at mother centrioles requires the step-wise removal of the daughter-specific CEP120, centrobin and Neurl4 in early S-phase to enable the recruitment of OFD1 (Wang et al., 2018). This first step is followed later, at around mitotic onset, with the progressive recruitment of other distal appendage proteins, including CEP164 (Fig. 3A). Thus, in a normal metaphase cell, OFD1 and CEP164 are present on both the grandmother and mother centriole. When looking at 1:1 cells

Journal of Cell Science (2022) 135, jcs259120. doi:10.1242/jcs.259120

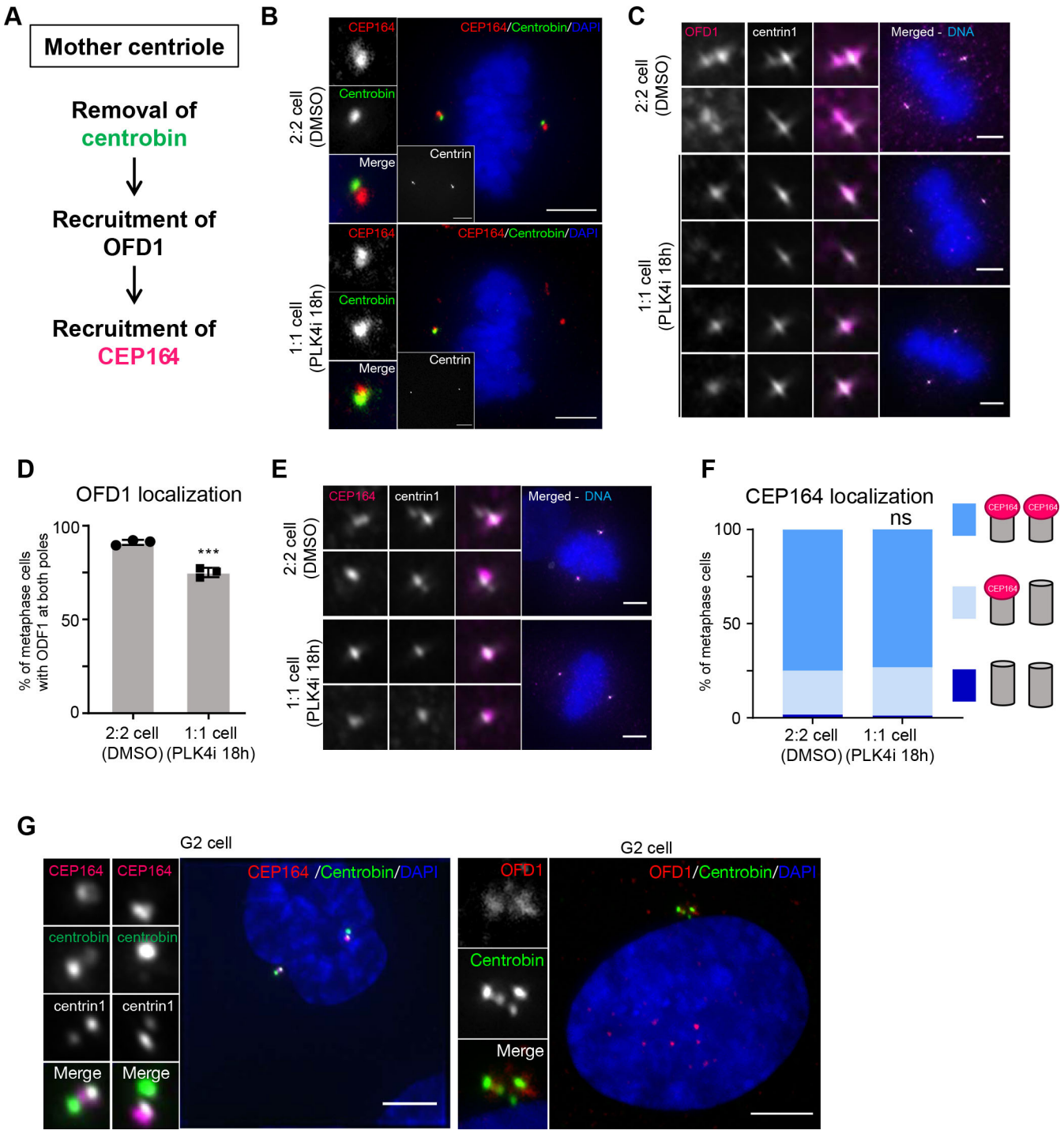

Fig. 3. Centrobin removal is not required for the recruitment of distal appendage proteins. (A) Model for the pathway controlling CEP164 recruitment on the mother centriole, as proposed by Wang et al. (2018). (B) Immunofluorescence images of hTert-RPE1-eGFP-centrin1 cells stained for CEP164 and centrobin, and treated with DMSO or with 250 nM PLK4 inhibitor for 18 h to obtain 1:1 cells. (C) Immunofluorescence images of metaphase hTertRPE1-eGFP-centrin1 cells stained with DAPI and OFD1 antibodies and treated either with DMSO or centrinone for 18 h. (D) Quantification of OFD1 localization pattern in 2:2 (*N*=3 independent experiments, *n*=146 cells) and 1:1 (*N*=3, *n*=118 cells) cells, ***P<0.001 (unpaired two-tailed Student's *t*-test). Error bars indicate s.e.m. (E) Immunofluorescence images of metaphase hTertRPE1-eGFP-centrin1 cells stained with DAPI and CEP164 antibodies, and treated either with DMSO or centrinone for 18 h. (F) Quantification of the CEP164 localization patterns in 2:2 (*N*=3, *n*=78 cells) and 1:1 (*N*=3, *n*=107 cells) metaphase hTertRPE1 eGFP-centrin1 cells. ns, not significant (two-way ANOVA with Tukey's multiple comparison test). (G) Immunofluorescence image of hTert-RPE1-eGFP-centrin1 G2 cell stained with antibodies against CEP164 and centrobin (left) or OFD1 and centrobin (right). Images shown in B and G are representative of three experiments. Scale bars: 5 µm.

that were co-stained with antibodies against centrobin and OFD1 or CEP164, we found that centrobin-positive mother centrioles were often also OFD1 or CEP164-positive (Figs 2F and 3B). This suggested that the presence of centrobin at the mother centriole in 1:1 cells did not perturb the recruitment of OFD1 or CEP164. Consistent with this, when we stained for OFD1 in a large number of

Journal of Cell Science (2022) 135, jcs259120. doi:10.1242/jcs.259120

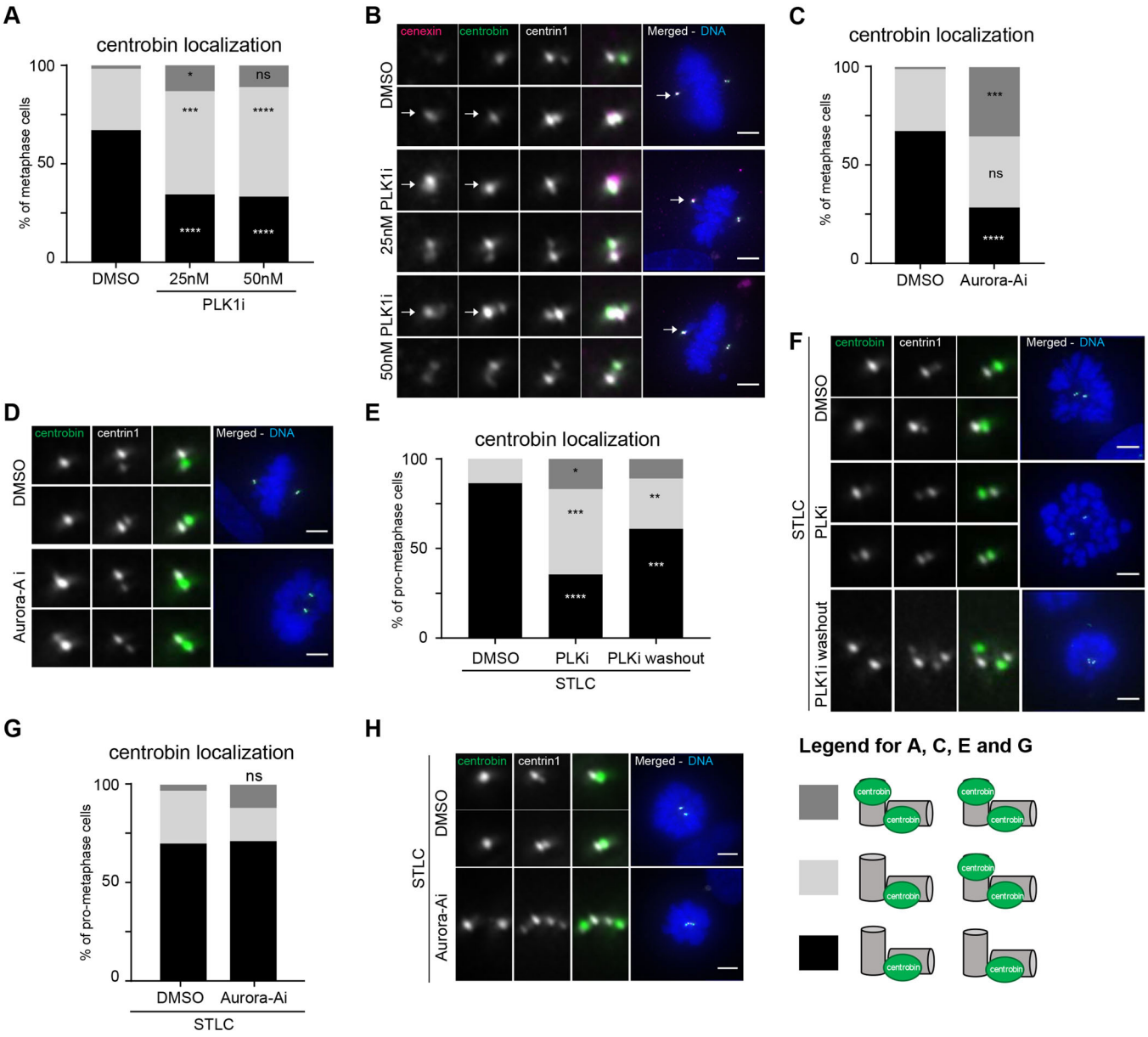

Fig. 4. Centrobin removal from mother centrioles depends on PLK1 activity. (A) Quantification of centrobin localization patterns in hTertRPE1-eGFP-centrin1 cells treated with DMSO (*N*=3 independent experiments, *n*=110 cells), 25 nM (*N*=3, *n*=115 cells) or 50 nM (*N*=3, *n*=125 cells) of the PLK1 inhibitor BI2536 for 2 h; **P*<0.05; ****P*<0.001; *****P*<0.0001; ns, not significant (two-way ANOVA with Tukey's multiple comparison test). (B) Immunofluorescence images of metaphase hTertRPE1-eGFP-centrin1 cells treated with DMSO, 25 nM or 50 nM of the PLK1 inhibitor BI2536 for 2 h and stained with DAPI and antibodies against cenexin and centrobin. White arrows label the old centrosome. (C) Quantification of centrobin localization patterns in hTertRPE1-eGFP-centrin1 cells treated with DMSO (*N*=3, *n*=110 cells), or the Aurora A inhibitor Alisertib (*N*=3, *n*=108 cells) for 2 h. ****P*<0.001, *****P*<0.0001; ns, not significant (two-way ANOVA with Tukey's multiple comparison test). (D) Immunofluorescence images of metaphase hTertRPE1-eGFP-centrin1 cells treated with DMSO or 100 nM Alisertib for 2 h and stained with DAPI and an antibody against centrobin. (E) Quantification of the centrobin localization patterns in hTertRPE1-eGFP-centrin1 cells arrested in prometaphase with STLC, treated either with DMSO for 4 h (*N*=3, 135 cells), with DMSO for 2 h and followed by 50 nM BI2536 for 2 h (PLK1i; *N*=3, *n*=130 cells), or with BI2536 for 2 h followed by DMSO for 2 h (PLKi washout; *N*=3, *n*=127 cells). **P*<0.05, ***P*<0.01, ****P*<0.001, *****P*<0.0001 (two-way ANOVA with Tukey's multiple comparison test). (F) Immunofluorescence images of prometaphase hTertRPE1-eGFP-centrin1 cells treated as described in E, and stained with DAPI and an antibody against centrobin. (G) Quantification of the centrobin localization patterns in hTertRPE1 eGFP-centrin1 cells arrested in prometaphase with STLC, treated either with DMSO for 4 h (*N*=3, *n*=140 cells), or with Alisertib for 4 h (*N*=3, *n*=87 cells). ns, not significant (two-way ANOVA with Tukey's multiple comparison test). (H) Immunofluorescence images of prometaphase hTertRPE1 eGFP-centrin1 cells treated as described in G and stained with DAPI and an antibody against centrobin. Scale bars: 5 µm.

1:1 cells, we found that a majority of them (75±2.5%; mean±s.e.m.) still displayed OFD1 at both grandmother and mother centrioles, as compared to 91±1.3% in 2:2 cells (Fig. 3C,D). CEP164 localization was even less affected, as it was present at grandmother and mother centrioles to the same extent in 2:2 and 1:1 cells (Fig. 3E,F). Consistent with the idea that the presence of centrobin is not incompatible with the loading of OFD1 and CEP164, we also even found examples of late G2 wild-type (WT) 2:2 cells in which CEP164 and centrobin or OFD1 and centrobin could be found on the same mother centriole (Fig. 3G).

Journal of Cell Science (2022) 135, jcs259120. doi:10.1242/jcs.259120

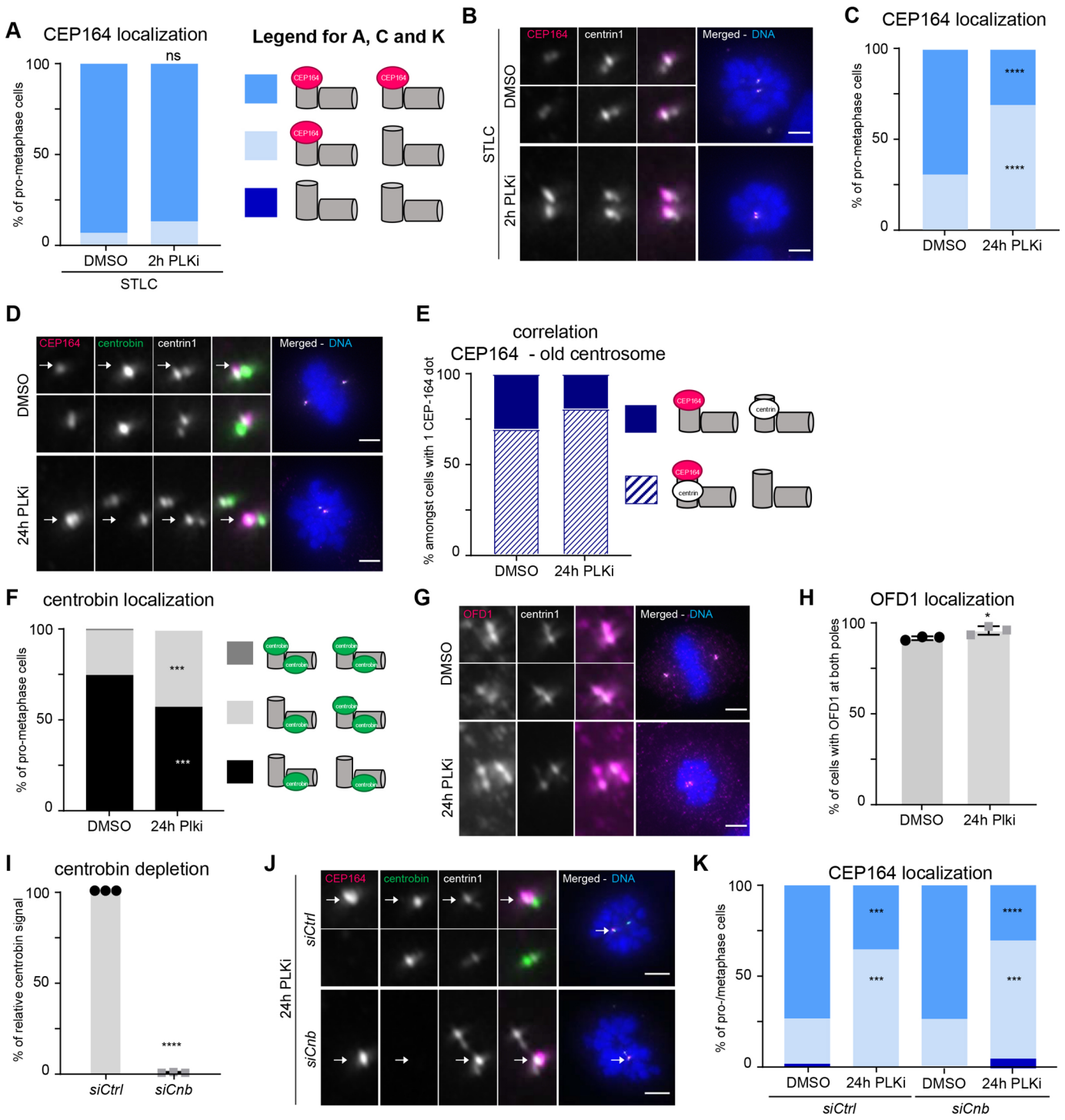

Fig. 5. See next page for legend.

PLK1 controls centrobin localization at centrosomes

In *Drosophila melanogaster* neuroblasts, the PLK1 kinase ortholog Polo controls the specific enrichment of centrobin on the younger centrosome (Gallaud et al., 2020; Januschke et al., 2013). We therefore tested whether mitotic phosphorylation also controls the removal of human centrobin in late prometaphase. Specifically, we tested the contribution of PLK1 and Aurora A, another key mitotic kinase controlling the centrosome cycle (Barr and Gergely, 2007). RPE eGFP–centrin1 cells were treated for 2 h with a either mock control (DMSO), 25 or 50 nM of the PLK1 inhibitor BI2536 (Lénárt et al., 2007), or 100 nM of the Aurora A inhibitor Alisertib (Görgün et al., 2010). Most control-treated cells (67±2%) displayed centrobin on the two daughter centrioles, whereas 32±2% (mean±s.e.m.) of the cells displayed three centrobin-positive centrioles (Fig. 4A,B). PLK1 inhibition increased the proportion of cells displaying a third centrobin-positive centriole to, respectively, 52±3% and 55±1%, and resulted in 10% of the cells with four centrobin-positive centrioles (Fig. 4A,B). After Aurora A inhibition, only 29±5% of the cells harbored centrobin at the two daughter centrioles, 36±5% on three centrioles, and 35±3% on all

Journal of Cell Science (2022) 135, jcs259120. doi:10.1242/jcs.259120

Fig. 5. PLK1 controls distal appendage protein recruitment and Centrobin removal via independent pathways. (A) Quantification of CEP164 localization patterns in hTertRPE1-eGFP-centrin1 cells treated with STLC in combination with 2 h DMSO (*N*=3 independent experiments, *n*=108 cells) or PLK1 inhibition with 50 nM BI 2356 (*N*=3, *n*=127 cells). (B) Immunofluorescence images of hTertRPE1-eGFP-centrin1 cells treated with STLC in combination with 2 h DMSO or PLK1 inhibition stained with DAPI and CEP164 antibodies. (C) Quantification of CEP164 localization patterns in hTertRPE1-eGFP-centrin1 cells treated with DMSO (*N*=3, *n*=143 cells) or 24 h PLK1 inhibition (*N*=3, *n*=113 cells). ****P<0.0001 (unpaired two-tailed Student's *t*-test). (D) Immunofluorescence images of hTertRPE1-eGFP-centrin1 cells treated with DMSO or 24 h PLK1 inhibition stained with DAPI and CEP164 antibodies. White arrows identify the old centrosome. (E) Correlation between single CEP164 presence and centrosome age based on eGFP–centrin1 signal in cells treated with DMSO (*N*=3, *n*=29 cells) or a PLK1 inhibitor (*N*=3, *n*=50 cells). (F) Quantification of centrobin localization patterns in hTertRPE1-eGFP-centrin1 cells treated with DMSO (*N*=3, *n*=143 cells) or 24 h PLK1 inhibition (*N*=3, *n*=113 cells). ***P<0.001 (unpaired two-tailed Student's *t*-test). (G) Immunofluorescence images of hTertRPE1 eGFP-centrin1 cells treated with DMSO or 24 h PLK1 inhibition stained with DAPI and OFD1 antibodies. (H) Quantification of OFD1 localization patterns in hTertRPE1 eGFP-centrin1 cells treated with DMSO (*N*=3, *n*=123 cells) or 24 h PLK1 inhibition (*N*=3, *n*=108 cells). *P<0.05 (unpaired two-tailed Student's *t*-test). Error bars indicate s.e.m. (I) Quantification of centrobin signal intensity after control (*N*=3, *n*=124 cells) or centrobin siRNA (*N*=3, *n*=140 cells). ****P<0.0001 (unpaired two-tailed Student's *t*-test). Error bars indicate s.e.m. (J) Immunofluorescence images of PLK1-inhibited (24 h) hTertRPE1 eGFP-centrin1 cells treated with control or centrobin siRNA, stained with DAPI and antibodies against CEP164 and centrobin. White arrows identify the old centrosome. (K) Quantification of CEP164 localization patterns in hTertRPE1-eGFP-centrin1 cells treated with DMSO plus control siRNA (*N*=3, *n*=126 cells), PLK1 inhibitor plus control siRNA (*N*=3, *n*=116 cells), DMSO plus centrobin siRNA (*N*=3, *n*=121 cells) or PLK1 inhibitor plus centrobin siRNA (*N*=3, *n*=108 cells). ***P<0.001, ****P<0.0001 comparing DMSO and PLK1-inhibition (two-way ANOVA with Tukey's multiple comparison test). Scale bars: 5 µm.

four centrioles (Fig. 4C,D). This indicated that centrobin removal from older centrioles depends both on PLK1 and Aurora A.

Since PLK1 is activated in G2 by Aurora-A to promote mitotic entry and centrosome separation (Seki et al., 2008), we next aimed to inhibit these two kinases only once cells had entered mitosis. We first arrested the cells in mitosis with STLC for 4 h, before inhibiting either PLK1 or Aurora-A for 2 h. STLC treatment and the resulting monopolar spindles did not affect centrobin localization, since we found the same pattern as in untreated cells – most mother centrioles had lost centrobin (Fig. 4E,F). PLK1 inhibition led to the rebinding of centrobin on older centrioles in STLC-treated cells, whereas Aurora A inhibition had no effect (Fig. 4G,H). This suggested: (1) that Aurora-A does not affect centrobin localization once PLK1 is fully active; (2) that PLK1 is the primary kinase controlling centrobin; and (3) that PLK1 inhibition can bring centrobin back to mother centrioles that had already lost it. To confirm the dynamicity of this regulation, we washed out BI2536 in STLC-treated cells after 2 h and replaced it either with DMSO or again BI2536. Washing out PLK1 inhibition restored normal centrobin localization on two centrioles, confirming the dynamic nature of this regulation in mitosis (Fig. 4E,F).

PLK1 regulates distal appendage formation independently of centrobin

Given that PLK1 activity also enables the recruitment of distal appendage proteins at the mother centriole (Kong et al., 2014), we next investigated the epistasis of this centrosome cycle step in relation to centrobin removal. Normally, CEP164 is present on both the grandmother and mother centriole in >90% of mitotic cells (Fig. 5A,B). Inhibition of PLK1 for 2 h in STLC treated cells did not disrupt CEP164 localization, if anything, it led to higher CEP164 levels at both centrioles (Fig. 5A,B). In contrast, PLK1 inhibition for 24 h resulted in 69±2% (mean±s.e.m.) of cells having CEP164 only at one centriole (Fig. 5C,D), consistent with a role of PLK1 in rendering centrioles compatible with the recruitment of distal appendage proteins (Kong et al., 2014). In the vast majority of cells, the CEP164-positive centriole was the grandmother centriole, identified by the higher intensity of the centrin1 signal (Fig. 5E; Tan et al., 2015). This suggests that PLK1 activity is required for the recruitment of CEP164 on the mother centriole prior to mitosis, but not for its maintenance during mitosis. Immunofluorescence analysis of cells treated with BI2536 for 24 h also indicated that centrobin was more frequently retained on the mother centriole (Fig. 5D,F). Nevertheless, OFD1 was present in 95±1% of cells on both spindle poles (versus 91±1% in control-treated cells; Fig. 5G,H). This confirmed that centrobin removal is not required as a pre-requisite for the loading of OFD1 on mother centriole and suggested that PLK1 controls CEP164 recruitment further downstream in the formation of distal appendages. To directly test whether PLK1 inhibition affects CEP164 recruitment via the presence of centrobin, we combined PLK1 inhibition with the siRNA-mediated depletion of centrobin. Although centrobin was efficiently depleted (Fig. 5I,J), its absence did not rescue the recruitment of CEP164 at the mother centriole; whether centrobin was present or not, PLK1 inhibition led to cells with only one CEP164-positive centriole in 64% of the cases (Fig. 5J,K). We conclude that PLK1 regulates the recruitment of CEP164 and the removal of centrobin via separate pathways.

Cenexin regulates recruitment of CEP164 and centrobin removal through separate pathways

Finally, we investigated the role of the core subdistal appendage protein cenexin in the regulation of the centrobin and the CEP164 pathways. Cenexin has been reported to modulate PLK1 activity at centrosomes (Colicino et al., 2019); moreover, in mouse embryonic F9 carcinoma cells, cenexin is required for the formation of both distal and subdistal appendages (Ishikawa et al., 2005; Tateishi et al., 2013). In RPE cells, however, it was reported to be only required for the formation of subdistal appendages (Kuhns et al., 2013; Tanos et al., 2013). While using two different siRNAs against cenexin to rule out any off-target effect, we found that efficient cenexin depletion (>80%, see Fig. S3A,B) led to the same configuration as the one seen after PLK1 inhibition in most cells: (1) only the grandmother centriole retained CEP164 (Fig. 6A,B, Fig. S3C; note that grandmother centrioles were identified based on the highest intensity of the eGFP-centrin1 signal); (2) centrobin was present on the mother centriole (Fig. 6C,D, Fig. S3D); and (3) OFD1 recruitment was not affected (Fig. 6E,F). This indicated that, as was the case for PLK1, cenexin is required for the removal of centrobin and the recruitment of CEP164 at the mother centriole, but that it does not affect OFD1 localization. To test for the epistasis of CEP164 recruitment and centrobin removal, we co-depleted both cenexin and centrobin and found that centrobin depletion did not rescue CEP164 binding to the mother centriole in cenexin-depleted cells (Fig. 6G,H; note that the co-depletions were as efficient as the single depletions; Fig. 3E–H). We conclude that cenexin regulates centrobin and CEP164 separately, and in an OFD1-independent manner.

We next extended our dependency analysis to the centrosomal proteins CEP128 and centriolin, which act downstream of cenexin in terms of building up subdistal appendages (Mazo et al., 2016). Using the published hTert-RPE1 cenexin, CEP128 or centriolin

Journal of Cell Science (2022) 135, jcs259120. doi:10.1242/jcs.259120

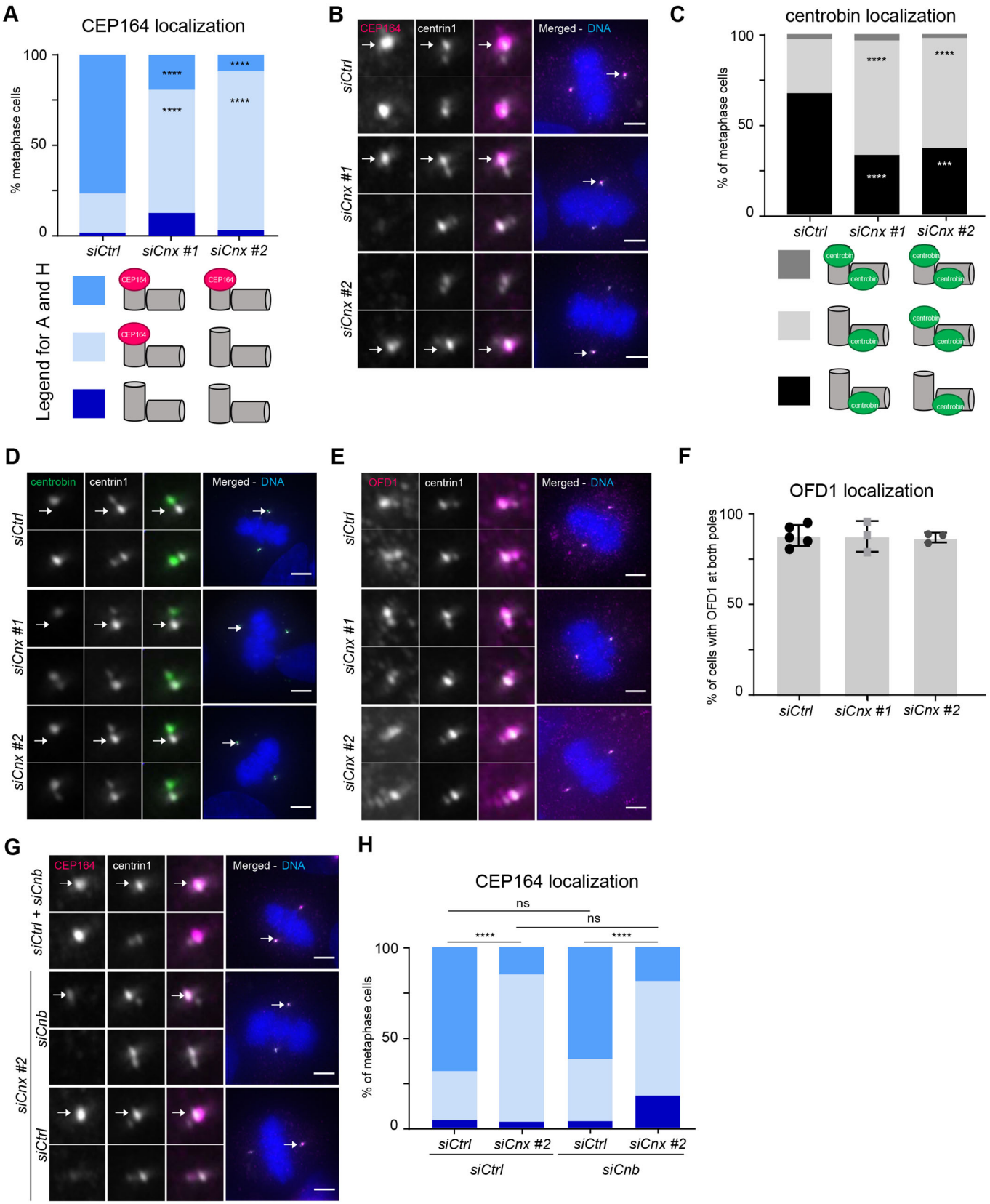

Fig. 6. See next page for legend.

Journal of Cell Science (2022) 135, jcs259120. doi:10.1242/jcs.259120

Fig. 6. Cenexin controls centrobin removal and distal appendage recruitment independently. (A) Quantification of CEP164 localization patterns in hTertRPE1-eGFP-centrin1 cells treated with either control siRNA (*N*=3 independent experiments, *n*=160 cells), cenexin siRNA #1 (*N*=3, *n*=124 cells) or cenexin siRNA #2 (*N*=3, *n*=132 cells), ****P<0.0001 (two-way ANOVA with Tukey's multiple comparison test). (B) Immunofluorescence images of hTertRPE1-eGFP-centrin1 cells treated with indicated siRNAs stained with DAPI and CEP164 antibodies. (C) Quantification of centrobin localization patterns in hTertRPE1-eGFP-centrin1 cells treated either control siRNA (*N*=3, *n*=160 cells), cenexin siRNA #1 (*N*=3, *n*=123 cells) or cenexin siRNA #2 (*N*=3, *n*=132 cells). ****P<0.0001, ***P<0.001 (two-way ANOVA with Tukey's multiple comparison test). (D,E) Immunofluorescence images of hTertRPE1-eGFP-centrin1 cells treated with the indicated siRNAs stained with DAPI and (D) centrobin or (E) OFD1 antibodies. (F) Quantification of OFD1 localization patterns in hTertRPE1-eGFP-centrin1 cells treated with indicated either control siRNA (*N*=3, *n*=194 cells), cenexin siRNA #1 (*N*=3, *n*=133 cells) or cenexin siRNA #2 (*N*=3, *n*=119 cells). Error bars indicate s.e.m.
(G) Immunofluorescence images of hTertRPE1-eGFP-centrin1 cells treated with indicated siRNAs, and stained with DAPI and CEP164 antibodies. White arrows identify the old centrosome. (H) Quantification of CEP164 localization patterns in hTertRPE1 eGFP-centrin1 cells treated with either control plus control siRNA (*N*=3, *n*=137 cells), control plus cenexin siRNA (*N*=3, *n*=136 cells), control plus centrobin siRNA (*N*=3, *n*=135 cells), cenexin plus centrobin siRNA (*N*=3, *n*=134 cells). ****P<0.0001; ns, not significant (two-way ANOVA with Tukey's multiple comparison test). Scale bars: 5 µm.

CRISPR/Cas9 knockout cell lines, we found that only cenexin deletion partially prevented the recruitment of CEP164, and that no defects could be seen in CEP128 or centriolin knockout cells (Fig. 7A,B; note that the percentage of cells with only one CEP164-positive centriole was lower compared to cenexin-depleted cells; see the Discussion). Our analysis further indicated that centrobin was present on all four centrioles in all three knockout cell lines, but that OFD1 localization was unchanged (Fig. 7C–F). The picture was more differentiated in G1 when only two centrioles are present (G1 cells were obtained by treating for 24 h with the CDK4 and CDK6 inhibitor palbociclib): in cenexin knockout cells, centrobin was present on both centrioles in 82% of the cells versus 18% in WT cells; in contrast in CEP128 and centriolin knock-out cells, centrobin was present on both centrioles in 60–63% of the cells, with a clear enrichment on the daughter centriole (Fig. S4A,B). We conclude that the mitotic removal of centrobin from older centrioles is not a pre-requisite for the recruitment of distal appendage proteins and that the removal of centrobin from maturing centrioles requires subdistal appendage proteins, in particular cenexin. In contrast, distal appendages, appear not to be required, since the depletion of the distal appendage protein CEP164 had no effect of centrobin localization (Fig. S4C–E).

DISCUSSION

In this present study, we investigated how the localization of the daughter-centriole-specific protein centrobin is controlled over the cell cycle in human epithelial cells, and whether centrobin acts as a placeholder protein for distal appendage proteins on the mother centriole. Our results imply that centrobin is removed from mother centriole in a dynamic manner and transferred on to daughter centrioles once cells reach mitosis, possibly due to a higher affinity. Centrobin removal requires the activity of the mitotic kinase PLK1 and the presence of subdistal appendage proteins on the mature centrioles. Finally, our results imply that centrobin does not act as a placeholder for the distal appendage proteins, but rather that centrobin removal and distal appendage protein recruitment are promoted by PLK1 via separate pathways.

Previous work in *Drosophila melanogaster* neuroblasts had shown that centrobin is transferred in metaphase in a PLK1-dependent manner from the mother centriole to the daughter centriole, potentially via a direct relocalization mechanism (Gallaud et al., 2020). Here, we show in human epithelial cells that removal from the mother centriole until metaphase is dynamic, as centrobin pools can co-exist on mother and daughter centrioles in G2, prophase and early prometaphase cells; moreover, we demonstrate that the presence of at least one daughter centriole is essential to remove centrobin from the mother centriole. Our quantification of centrobin pools on mother centrioles in 1:1 cells, on normal daughter centrioles in 2:2 cells and in cells with extra daughter centrioles lead us to propose a speculative model in which higher-affinity binding sites on daughter centrioles compete against weaker-affinity binding sites on mother centrioles for a dynamic but limited centrobin pool that is rapidly exchanged via the cytoplasm. In such a model, as centrobin is dynamically exchanged with the cytoplasm, it will gradually leave mother centrioles and accumulate on maturating daughter centrioles; if daughter centrioles are absent, centrobin will remain on mother centrioles. We emphasize, however, that demonstrating such an affinity model will require more direct biochemical evidence with recombinant proteins and purified centrioles.

Although our data indicate that PLK1 inhibition leads to a reversible association of centrobin to the mother centriole, it is unclear at which level this kinase acts. In theory PLK1 activity could decrease the affinity of the centrobin-binding site on the mother centriole, increase it on the daughter centrioles, or switch the binding preference by directly phosphorylating centrobin itself, in line with the fact that centrobin is a PLK1 substrate (Lee et al., 2010). Our present resolution also does not allow us to distinguish whether, in PLK1 inhibited cells, centrobin re-associates to the same distal end of mother centrioles as control S-phase cells. The subdistal appendage proteins cenexin, CEP128 and centriolin, which in metaphase are predominantly present at the grandmother centriole (Colicino et al., 2019; Gasic et al., 2015; Ishikawa et al., 2005; Kong et al., 2014), are also required or contribute to centrobin removal from the mother centriole. Given the vast distances between the two spindle poles at this stage, this control is most likely indirect, although one cannot completely exclude that subdistal appendages on the grandmother centriole may affect the mother centriole in the preceding interphase. One likely pathway is that the subdistal appendages regulate PLK1 activity, consistent with previous studies showing that the presence of cenexin enhances PLK1 activity (Colicino et al., 2019); whether CEP128 and centriolin play a similar role, remains to be investigated.

Finally, our results indicate that centrobin does not act as a placeholder for distal appendage proteins, in contrast to a previously proposed model (Wang et al., 2018). Our data identify multiple experimental conditions in which centrobin presence at mother centriole does not prevent the recruitment of OFD1, which is recruited early, and of CEP164, which is recruited last during distal appendage formation. This co-existence can even be seen in WT G2 cells, with examples of centrobin-positive mother centrioles that have already begun to recruit OFD1 or even CEP164. Our investigation of subdistal appendage proteins further indicates that cenexin is partially required for the presence of CEP164, but not of OFD1, on the mother centriole in metaphase. This role is specific for cenexin, as knockouts of CEP128 and centriolin did not reveal any changes in CEP164 localization, confirming that centrobin removal and CEP164 recruitment are independent. We further note that the acute depletion of cenexin by both tested siRNAs, even when not fully effective, led to a stronger reduction in CEP164 levels on metaphase mother centrioles than in the cenexin knockout cells. This could

Journal of Cell Science (2022) 135, jcs259120. doi:10.1242/jcs.259120

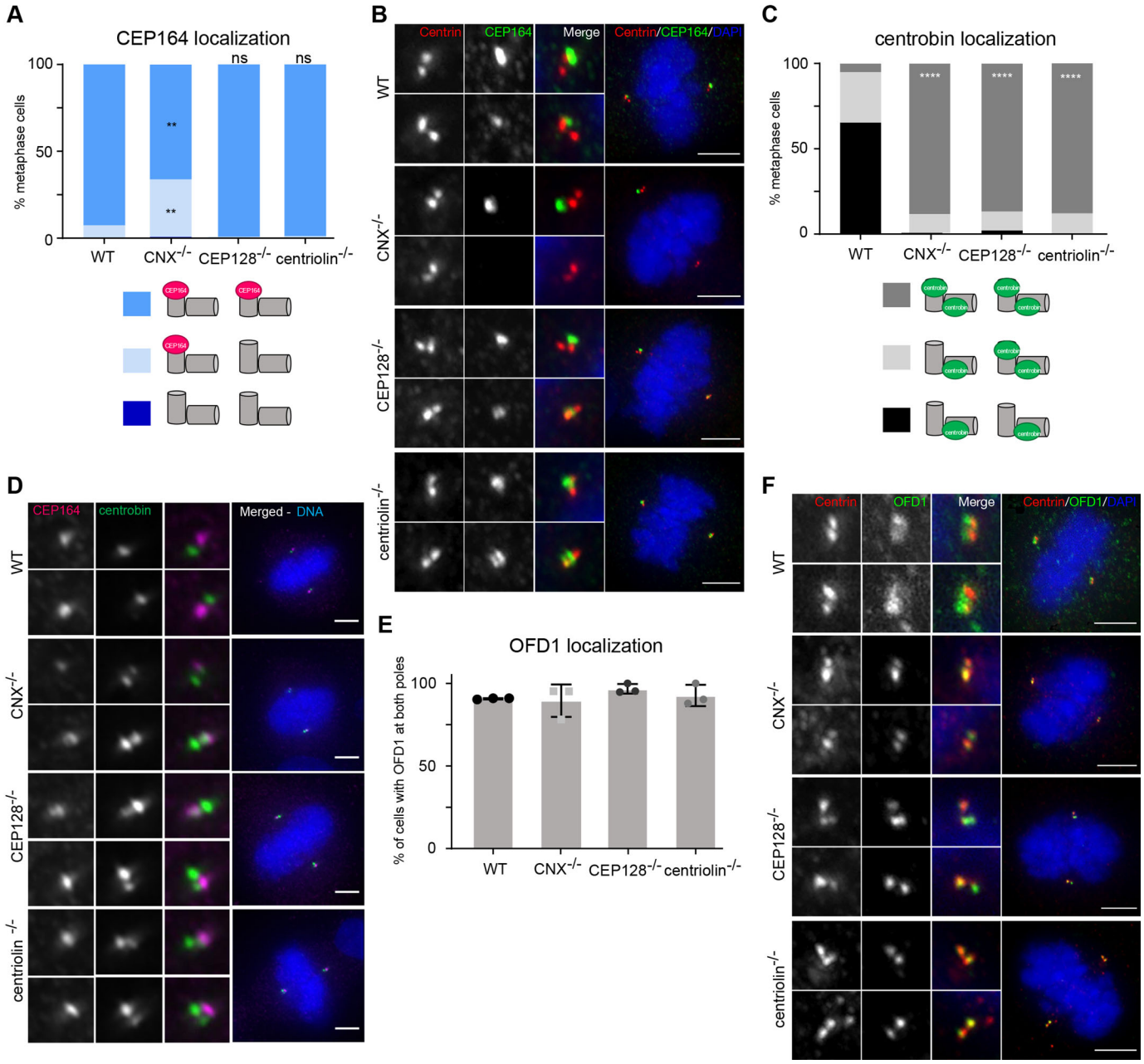

Fig. 7. Subdistal appendages are required for centrobin removal, but not for distal appendage assembly. (A) Quantification of CEP164 localization patterns in the parental WT hTertRPE1 cells (*N*=3 independent experiments, *n*=141 cells) and cenexin (*N*=3, *n*=155 cells), CEP128 (*N*=3, *n*=119 cells) or centriolin (*N*=3, *n*=130 cells) knockout cells. ***P*<0.01; ns, not significant (two-way ANOVA with Tukey's multiple comparison test). (B) Immunofluorescence images of WT or respective knockout metaphase hTert-RPE1 cells stained with DAPI and antibodies against CEP164 and centrin1. (C) Quantification of the centrobin localization patterns in the parental WT hTertRPE1 cell (*N*=3, *n*=141 cells) and cenexin (*N*=3, *n*=154 cells), CEP128 (*N*=3, *n*=119 cells) or centriolin (*N*=3, *n*=130 cells) knockout cells. *****P*<0.0001; ns, not significant (two-way ANOVA with Tukey's multiple comparison test). (D) Immunofluorescence images of indicated hTertRPE1 cells stained with DAPI and antibodies against CEP164 and centrobin. (E) Quantification of OFD1 localization patterns in the parental WT hTertRPE1 cell (*n*=129 cells) and cenexin (*n*=115 cells), CEP128 (*n*=119 cells) or centriolin (*n*=122 cells) knockouts. Error bars indicate s.e.m. (F) Immunofluorescence images of indicated hTert-RPE1 cells stained with DAPI and antibodies against OFD1 and centrin1. Scale bars: 5 µm.

suggest that knockout cells have adapted to cenexin loss, as has been seen for other deletions (Rossi et al., 2015), allowing them to nevertheless efficiently form distal appendages. Finally, our data confirm that the presence of CEP164 at mother centrioles in metaphase requires PLK1 activity, as seen in other studies (Kong et al., 2014; Tanos et al., 2013). This dependency is, however, only transient, since PLK1 inhibition does not affect the maintenance of distal appendages at later stages. This is consistent with the idea that PLK1 enables distal appendage protein recruitment on the mother centriole by promoting centriole maturation (Kong et al., 2014). It also fits with the idea that distal appendage formation does not solely depend on PLK1 but is under the complex control of several other centrosomal kinases, such as Nek2 and Aurora A (Bowler et al., 2019; Viol et al., 2020). Overall, we postulate that, in human epithelial cells, PLK1 controls centriole maturation via separate pathways, one involving centrobin removal, the second enabling recruitment of distal appendage proteins on the mother centriole. This raises the question of the reasons for centrobin removal since its

Journal of Cell Science

Journal of Cell Science (2022) 135, jcs259120. doi:10.1242/jcs.259120

presence does not impact distal appendage formation. In *Drosophila* neuroblasts, centrobin localization has to be controlled since it regulates the fate of the young centrosome, enabling it to organize microtubules and to be retained by the stem cell during asymmetric cell division (Januschke et al., 2013). In mammalian cells, however, the reasons for controlling centrobin still remain to be uncovered. Our characterization of 1:1 cells indicate that the presence of centrobin at the mother centriole on one pole neither affects mitotic progression nor change the incidence of chromosome segregation errors, indicating that its removal is not acutely necessary for centrosome or spindle pole function in mitosis. Rather, we speculate that timely removal of centrobin in (pro-)metaphase might be linked to the precision of centriole elongation during the centrosome duplication cycle and to cilia formation, since it has been shown that overexpressing centrobin leads to overelongated centrioles and may affect the axoneme structure during ciliogenesis (Gudi et al., 2015; Ogungbenro et al., 2018).

MATERIALS AND METHODS

Cell culture and drug treatments

hTERT-RPE1 cells, hTERT-RPE1 eGFP-centrin1 cells, hTERT-RPE1 eGFP-Centrin1/eGFP-CENP-A cells (both gifts of Alexey Khodjakov, New York State Department of Health, Wadsworth Center, USA; Magidson et al., 2011), hTERT-RPE1 cenexin knockout cells, Cep128 knockout cells, centriolin knockout cells and their parental cell line (gift of Brian Tsou, Memorial Sloan Kettering Cancer Center, Sloan Kettering Institute, USA; Mazo et al., 2016), were all grown in Dulbecco's modified Eagle's medium (DMEM; Thermo Fisher Scientific, Switzerland), supplemented with 10% fetal calf serum (FCS), 100 U/ml penicillin, and 100 mg/ml streptomycin (all Life Technologies, Switzerland) at 37°C and 5% CO_2. All cell lines were regularly tested for contamination. For live-cell imaging, cells were kept in their normal medium if a CO_2 chamber was used, or otherwise cultured in Leibovitz's L-15 medium without Phenol Red (Thermo Fisher Scientific), supplemented with 5% FCS. To inhibit PLK1, 25 nM or 50 nM BI2536 (Axon Lab AG, Switzerland) was used, for either 2 h or 24 h. To inhibit Aurora-A, 100 nM Alisertib (Selleckchem, USA) was used for 2 h. For the PLK1 inhibition washout experiments, cells were treated with 5 µM STLC for 4 h to maintain them in prometaphase, 50 nM BI2536 was added for 2 h before adding back medium containing only STLC for 2 h. To obtain 1:1 cells, cells were treated with 250 nM centrinone (a PLK4 inhibitor; Tocris, UK) for 18 h. To obtain cells with excessive numbers of daughter centrioles, cells were treated with a partial dose (25 nM) of centrinone for 30 h. Alternatively, a short 2 h treatment was added as a negative control. To obtain WT cells, cenexin knockout, CEP128 or centriolin knockout cells in G1 phase, cells were treated for 24 h with the CDK4 and CDK6 inhibitor Palbociclib (Sigma-Aldrich, Switzerland).

SiRNA-mediated protein depletions

In general siRNA treatments were performed for 48 h by applying 40 nmol siRNAs and 1% Lipofectamine RNAimax (Invitrogen) following the manufacturer's protocol. To deplete cenexin, we applied 180 nmol siRNA and 3% Lipofectamine RNAimax (Invitrogen) instead; to prevent centriole duplication and obtain a mix of 2:1 and 1:1 cells, Sas-6 was depleted for only 24 h. The target sequences of the siRNAs used are: *siCEP164* (mix of 5′-CAGGTGACATTTACTATTTCA-3′ and 5′-ACCACTGGGAATAGA-AGACAA-3′), *siCnb* (mix of 5′-TGGAAATGGCAGAACGAGA-3′, 5′-GCATGAGGCTGAGCGGACA-3′, 5′-GCCCAAGAATTGAGTCG-AA-3′ and 5′-CTCCAAACCTCACGTGATA-3′), *siCnx #1* (5′-TGGC-TGAGACTGAGCACGA-3′), *siCnx #2* (5′-GGCACAACATCGAGCG-CAT-3′), siCtrl (5′-AAGGACCTGGAGGTCTGCTGT-3′) and *siSas-6* (5′-GCACGTTAATCAGCTACAA-3′).

Immunofluorescence

Cells were grown on acid-etched glass coverslips and either fixed for 6 min at −20°C with ice-cold methanol, or for 15 min with a formaldehyde fixative (0.05 M PIPES, 0.01 M EGTA, 1 mM $MgCl_2$, 0,2% Triton X-100 and 4% formaldehyde) at room temperature. Coverslips were washed with phosphate-buffered saline solution (PBS) three times before adding a blocking buffer for 1 h at room temperature (7.5% bovine serum albumin, 0.25% sodium azide in PBS). Primary antibodies were diluted in blocking buffer and added for 1 h at room temperature followed by three PBS washes. The following primary antibodies were used: rabbit anti-cenexin (1:1000, Abcam, UK, ab43840), goat anti-cenexin (1:1000, Abcam, ab121023), mouse anti-centrin1 (1:2000, clone 20H5 Merck Millipore, Switzerland), mouse anti-centrobin (1:1000, Abcam ab70448) or, alternatively, mouse-anti-centrobin (1:1000 Sigma-Aldrich, SAB1408254), mouse anti-Sas6 (1:200, Santa Cruz Biotechnology, USA, sc-81431), rabbit anti-CEP164 (1:1000, gift of Erich Nigg, Biozentrum Basel, University of Basel, Switzerland; Graser et al., 2007), rabbit anti-OFD1 (1:1000, Abcam ab222837), mouse anti-pericentrin (1:1000, Abcam ab28144), rabbit anti-γ-tubulin (1:2000; Wilhelm et al., 2019), and rabbit anti-PCNA (1:1000, Abcam ab18197). Cross-absorbed secondary antibodies tagged with Alexa Fluor fluorophores were diluted in blocking buffer (1:400, Invitrogen, Switzerland) and applied for 30 min at room temperature. Vectashield with DAPI (Vector Laboratories, Switzerland) was used to mount the coverslips, and images were taken with a wide-field Olympus Deltavision (GE Healthcare, USA), with a 60×1.4 NA oil objective and a DAPI/FITC/TRITC/Cy5 (Chroma, USA) filter set. The *z*-stack images were recorded in 0.2 µm steps with a Coolsnap HQ2 CCD camera (Roper Scientific) and the Softworx software (GE Healthcare). Image stacks were deconvolved and protein levels at centrioles were quantified based on maximal intensity projections using Softworx Explorer (GE Healthcare). To quantify pericentriolar protein levels, we applied with Imaris (Bitplane, Switzerland) a 0.5 µm diameter sphere centered on the eGFP–centrin1 signal and quantified the summed intensity within this sphere.

Readout for centrosome age

In most of the experiments, cenexin signal was used to identify the grandmother centriole, and therefore which centrosome was the old one. For experiments where cenexin was depleted and for experiments performed with RPE cells knocked out for cenexin, CEP128 or centriolin, centrin1 signal was used as a readout (Gasic et al., 2015), and only cells with a difference higher than 5% in centrin1 signal between the two centrosomes were analyzed. This difference was calculated with the following formula:

$$\text{Difference} = \frac{\left|(\text{Centrin signal} - \text{Background})_{\text{centrosome 1}} - (\text{Centrin signal} - \text{Background})_{\text{centrosome 2}}\right|}{(\text{Centrin signal} - \text{Background})_{\text{centrosome 1}} + (\text{Centrin signal} - \text{Background})_{\text{centrosome 2}}} \times 100.$$

Centrin was also used to distinguish between the old and young centrosomes in experiments where CEP164 localization was studied.

Statistical analysis

The data is presented as the mean of multiple independent experiments and error bars represent the s.e.m. unless otherwise specified. Significance was determined using Graphpad Prism, and are represented presented in this work according to the following codification: *P<0.05, **P<0.01, ***P<0.001 and ****P<0.0001. An unpaired two-tailed *t*-test assessed the depletion efficiency for cenexin, centrobin or CEP164. For all the data describing the changes in centrobin and CEP164 localization, a two-way ANOVA with Tukey's multiple comparison test was chosen. For the comparison of the relative centrobin levels on grandmother, mother and daughter centrioles a one-way ANOVA test with Sidak's multiple comparison test was applied. All illustrations and graphs were created using ImageJ Fiji, Graphpad Prism and Adobe Illustrator.

Acknowledgements

Authors are grateful to A. McAinsh (University of Warwick, UK), A. Khodjakov (NY State University, USA), B. Tsou (Cornell University, NY, USA) for cell lines, E. Nigg (University of Basel, Switzerland) for CEP164 antibodies, Monica Gotta (University of Geneva, Switzerland) and members of the Meraldi laboratory for helpful discussions and support, especially E. Galster for her help in cell lines' maintenance

and A.-M. Olziersky, L. Romanens, D. Dudka, and T. Wilhelm for critical comments on the manuscript.

Competing interests
The authors declare no competing or financial interests.

Author contributions
Conceptualization: M.L.R.-B., P.M.; Formal analysis: M.L.R.-B., D.D., P.M.; Investigation: M.L.R.-B., D.D., D.H.; Writing - original draft: M.L.R.-B.; Writing - review & editing: M.L., D.D., P.M.; Visualization: M.L.R.-B., D.D.; Supervision: P.M.; Project administration: P.M.; Funding acquisition: P.M.

Funding
This work was supported by the Swiss National Science Foundation (Schweizerischer Nationalfonds zur Förderung der Wissenschaftlichen Forschung; SNF) project grant (No. 31003A_179413) and the Université de Genève.

Data availability
The secondary data from this publication is available from https://doi.org/10.26037/yareta:hjffjrpzqfewzdfo24vsxe3ruu. For the very large datasets of primary data, please contact the authors who will send them to you on external hard disks.

Peer review history
The peer review history is available online at https://journals.biologists.com/jcs/article-lookup/doi/10.1242/jcs.259120.

References
Barr, A. R. and Gergely, F. (2007). Aurora-A: the maker and breaker of spindle poles. *J. Cell Sci.* **120**, 2987-2996. doi:10.1242/jcs.013136

Bornens, M. (2002). Centrosome composition and microtubule anchoring mechanisms. *Curr. Opin. Cell Biol.* **14**, 25-34. doi:10.1016/S0955-0674(01)00290-3

Bowler, M., Kong, D., Sun, S., Nanjundappa, R., Evans, L., Farmer, V., Holland, A., Mahjoub, M. R., Sui, H. and Loncarek, J. (2019). High-resolution characterization of centriole distal appendage morphology and dynamics by correlative STORM and electron microscopy. *Nat. Commun.* **10**, 993. doi:10.1038/s41467-018-08216-4

Chong, W. M., Wang, W.-J., Lo, C.-H., Chiu, T.-Y., Chang, T.-J., Liu, Y.-P., Tanos, B., Mazo, G., Tsou, M.-F. B., Jane, W.-N. et al. (2020). Super-resolution microscopy reveals coupling between mammalian centriole subdistal appendages and distal appendages. *Elife* **9**, e53580. doi:10.7554/eLife.53580.sa2

Colicino, E. G., Stevens, K., Curtis, E., Rathbun, L., Bates, M., Manikas, J., Amack, J., Freshour, J. and Hehnly, H. (2019). Chromosome misalignment is associated with PLK1 activity at cenexin-positive mitotic centrosomes. *Mol. Biol. Cell* **30**, 1598-1609. doi:10.1091/mbc.E18-12-0817

DeBonis, S., Skoufias, D. A., Lebeau, L., Lopez, R., Robin, G., Margolis, R. L., Wade, R. H. and Kozielski, F. (2004). In vitro screening for inhibitors of the human mitotic kinesin Eg5 with antimitotic and antitumor activities. *Mol. Cancer Ther.* **3**, 1079-1090.

Delgehyr, N., Sillibourne, J. and Bornens, M. (2005). Microtubule nucleation and anchoring at the centrosome are independent processes linked by ninein function. *J. Cell Sci.* **118**, 1565-1575. doi:10.1242/jcs.02302

Dudka, D., Castrogiovanni, C., Liaudet, N., Vassal, H. and Meraldi, P. (2019). Spindle-length-dependent HURP localization allows centrosomes to control kinetochore-fiber plus-end dynamics. *Curr. Biol.* **29**, 3563-3578. doi:10.1016/j.cub.2019.08.061

Gallaud, E., Ramdas Nair, A., Horsley, N., Monnard, A., Singh, P., Pham, T. T., Salvador Garcia, D., Ferrand, A. and Cabernard, C. (2020). Dynamic centriolar localization of Polo and Centrobin in early mitosis primes centrosome asymmetry. *PLoS Biol.* **18**, e3000762. doi:10.1371/journal.pbio.3000762

Gasic, I., Nerurkar, P. and Meraldi, P. (2015). Centrosome age regulates kinetochore microtubule stability and biases chromosome mis-segregation. *Elife* **4**, e07909. doi:10.7554/eLife.07909

Gönczy, P. and Hatzopoulos, G. N. (2019). Centriole assembly at a glance. *J. Cell Sci.* **132**, jcs228833. doi:10.1242/jcs.228833

Görgün, G., Calabrese, E., Hideshima, T., Ecsedy, J., Perrone, G., Mani, M., Ikeda, H., Bianchi, G., Hu, Y., Cirstea, D. et al. (2010). A novel Aurora-A kinase inhibitor MLN8237 induces cytotoxicity and cell-cycle arrest in multiple myeloma. *Blood* **115**, 5202-5213. doi:10.1182/blood-2009-12-259523

Gottardo, M., Pollarolo, G., Llamazares, S., Reina, J., Riparbelli, M. G., Callaini, G. and Gonzalez, C. (2015). Loss of centrobin enables daughter centrioles to form sensory cilia in drosophila. *Curr. Biol.* **25**, 2319-2324. doi:10.1016/j.cub.2015.07.038

Graser, S., Stierhof, Y.-D., Lavoie, S. B., Gassner, O. S., Lamla, S., Le Clech, M. and Nigg, E. A. (2007). Cep164, a novel centriole appendage protein required for primary cilium formation. *J. Cell Biol.* **179**, 321-330. doi:10.1083/jcb.200707181

Guderian, G., Westendorf, J., Uldschmid, A. and Nigg, E. A. (2010). Plk4 trans-autophosphorylation regulates centriole number by controlling betaTrCP-mediated degradation. *J. Cell Sci.* **123**, 2163-2169. doi:10.1242/jcs.068502

Gudi, R., Zou, C., Dhar, J., Gao, Q. and Vasu, C. (2014). Centrobin-centrosomal protein 4.1-associated protein (CPAP) interaction promotes CPAP localization to the centrioles during centriole duplication. *J. Biol. Chem.* **289**, 15166-15178. doi:10.1074/jbc.M113.531152

Gudi, R., Haycraft, C. J., Bell, P. D., Li, Z. and Vasu, C. (2015). Centrobin-mediated regulation of the centrosomal protein 4.1-associated protein (CPAP) level limits centriole length during elongation stage. *J. Biol. Chem.* **290**, 6890-6902. doi:10.1074/jbc.M114.603423

Ishikawa, H., Kubo, A., Tsukita, S. and Tsukita, S. (2005). Odf2-deficient mother centrioles lack distal/subdistal appendages and the ability to generate primary cilia. *Nat. Cell Biol.* **7**, 517-524. doi:10.1038/ncb1251

Januschke, J., Llamazares, S., Reina, J. and Gonzalez, C. (2011). Drosophila neuroblasts retain the daughter centrosome. *Nat. Commun.* **2**, 243. doi:10.1038/ncomms1245

Januschke, J., Reina, J., Llamazares, S., Bertran, T., Rossi, F., Roig, J. and Gonzalez, C. (2013). Centrobin controls mother-daughter centriole asymmetry in Drosophila neuroblasts. *Nat. Cell Biol.* **15**, 241-248. doi:10.1038/ncb2671

Kong, D., Farmer, V., Shukla, A., James, J., Gruskin, R., Kiriyama, S. and Loncarek, J. (2014). Centriole maturation requires regulated Plk1 activity during two consecutive cell cycles. *J. Cell Biol.* **206**, 855-865. doi:10.1083/jcb.201407087

Kuhns, S., Schmidt, K. N., Reymann, J., Gilbert, D. F., Neuner, A., Hub, B., Carvalho, R., Wiedemann, P., Zentgraf, H., Erfle, H. et al. (2013). The microtubule affinity regulating kinase MARK4 promotes axoneme extension during early ciliogenesis. *J. Cell Biol.* **200**, 505-522. doi:10.1083/jcb.201206013

Lange, B. M. and Gull, K. (1995). A molecular marker for centriole maturation in the mammalian cell cycle. *J. Cell Biol.* **130**, 919-927. doi:10.1083/jcb.130.4.919

Lee, J., Jeong, Y., Jeong, S. and Rhee, K. (2010). Centrobin/NIP2 is a microtubule stabilizer whose activity is enhanced by PLK1 phosphorylation during mitosis. *J. Biol. Chem.* **285**, 25476-25484. doi:10.1074/jbc.M109.099127

Leidel, S., Delattre, M., Cerutti, L., Baumer, K. and Gönczy, P. (2005). SAS-6 defines a protein family required for centrosome duplication in C. elegans and in human cells. *Nat. Cell Biol.* **7**, 115-125. doi:10.1038/ncb1220

Lénárt, P., Petronczki, M., Steegmaier, M., Di Fiore, B., Lipp, J. J., Hoffmann, M., Rettig, W. J., Kraut, N. and Peters, J.-M. (2007). The small-molecule inhibitor BI 2536 reveals novel insights into mitotic roles of polo-like kinase 1. *Curr. Biol.* **17**, 304-315. doi:10.1016/j.cub.2006.12.046

Loncarek, J. and Bettencourt-Dias, M. (2018). Building the right centriole for each cell type. *J. Cell Biol.* **217**, 823-835. doi:10.1083/jcb.201704093

Magidson, V., O'Connell, C. B., Loncarek, J., Paul, R., Mogilner, A. and Khodjakov, A. L. (2011). The spatial arrangement of chromosomes during prometaphase facilitates spindle assembly. *Cell* **146**, 555-567. doi:10.1016/j.cell.2011.07.012

Mazo, G., Soplop, N., Wang, W.-J., Uryu, K. and Tsou, M.-F. B. (2016). Spatial control of primary ciliogenesis by subdistal appendages alters sensation-associated properties of cilia. *Dev. Cell* **39**, 424-437. doi:10.1016/j.devcel.2016.10.006

Ogungbenro, Y. A., Tena, T. C., Gaboriau, D., Lalor, P., Dockery, P., Philipp, M. and Morrison, C. G. (2018). Centrobin controls primary ciliogenesis in vertebrates. *J. Cell Biol.* **217**, 1205-1215. doi:10.1083/jcb.201706095

Reina, J., Gottardo, M., Riparbelli, M. G., Llamazares, S., Callaini, G. and Gonzalez, C. (2018). Centrobin is essential for C-tubule assembly and flagellum development in Drosophila melanogaster spermatogenesis. *J. Cell Biol.* **217**, 2365-2372. doi:10.1083/jcb.201801032

Rossi, A., Kontarakis, Z., Gerri, C., Nolte, H., Hölper, S., Krüger, M. and Stainier, D. Y. R. (2015). Genetic compensation induced by deleterious mutations but not gene knockdowns. *Nature* **524**, 230-233. doi:10.1038/nature14580

Seki, A., Coppinger, J. A., Jang, C.-Y., Yates, J. R. and Fang, G. (2008). Bora and the kinase Aurora a cooperatively activate the kinase Plk1 and control mitotic entry. *Science* **320**, 1655-1658. doi:10.1126/science.1157425

Singla, V., Romaguera-Ros, M., Garcia-Verdugo, J. M. and Reiter, J. F. (2010). Ofd1, a human disease gene, regulates the length and distal structure of centrioles. *Dev. Cell* **18**, 410-424. doi:10.1016/j.devcel.2009.12.022

Tan, C. H., Gasic, I., Huber-Reggi, S. P., Dudka, D., Barisic, M., Maiato, H. and Meraldi, P. (2015). The equatorial position of the metaphase plate ensures symmetric cell divisions. *Elife* **4**, e05124. doi:10.7554/eLife.05124

Tanos, B. E., Yang, H.-J., Soni, R., Wang, W.-J., Macaluso, F. P., Asara, J. M. and Tsou, M.-F. B. (2013). Centriole distal appendages promote membrane docking, leading to cilia initiation. *Genes Dev.* **27**, 163-168. doi:10.1101/gad.207043.112

Tateishi, K., Yamazaki, Y., Nishida, T., Watanabe, S., Kunimoto, K., Ishikawa, H. and Tsukita, S. (2013). Two appendages homologous between basal bodies and centrioles are formed using distinct Odf2 domains. *J. Cell Biol.* **203**, 417-425. doi:10.1083/jcb.201303071

Tischer, J., Carden, S. and Gergely, F. (2021). Accessorizing the centrosome: new insights into centriolar appendages and satellites. *Curr. Opin. Struct. Biol.* **66**, 148-155. doi:10.1016/j.sbi.2020.10.021

Vásquez-Limeta, A. and Loncarek, J. (2021). Human centrosome organization and function in interphase and mitosis. *Semin. Cell Dev. Biol.* **117**, 30-41. doi:10.1016/j.semcdb.2021.03.020

Viol, L., Hata, S., Pastor Peidro, A., Neuner, A., Murke, F., Wuchter, P., Ho, A. D., Giebel, B. and Pereira, G. (2020). Nek2 kinase displaces distal appendages from the mother centriole prior to mitosis. *J. Cell Biol.* **219**, e201907136. doi:10.1083/jcb.201907136

Wang, L., Failler, M., Fu, W. and Dynlacht, B. D. (2018). A distal centriolar protein network controls organelle maturation and asymmetry. *Nat. Commun.* **9**, 3938. doi:10.1038/s41467-018-06286-y

Wilhelm, T., Olziersky, A.-M., Harry, D., De Sousa, F., Vassal, H., Eskat, A. and Meraldi, P. (2019). Mild replication stress causes chromosome mis-segregation via premature centriole disengagement. *Nat. Commun.* **10**, 3585. doi:10.1038/s41467-019-11584-0

Wong, Y. L., Anzola, J. V., Davis, R. L., Yoon, M., Motamedi, A., Kroll, A., Seo, C. P., Hsia, J. E., Kim, S. K., Mitchell, J. W. et al. (2015). Cell biology. Reversible centriole depletion with an inhibitor of Polo-like kinase 4. *Science* **348**, 1155-1160. doi:10.1126/science.aaa5111

Zou, C., Li, J., Bai, Y., Gunning, W. T., Wazer, D. E., Band, V. and Gao, Q. (2005). Centrobin: a novel daughter centriole-associated protein that is required for centriole duplication. *J. Cell Biol.* **171**, 437-445. doi:10.1083/jcb.200506185

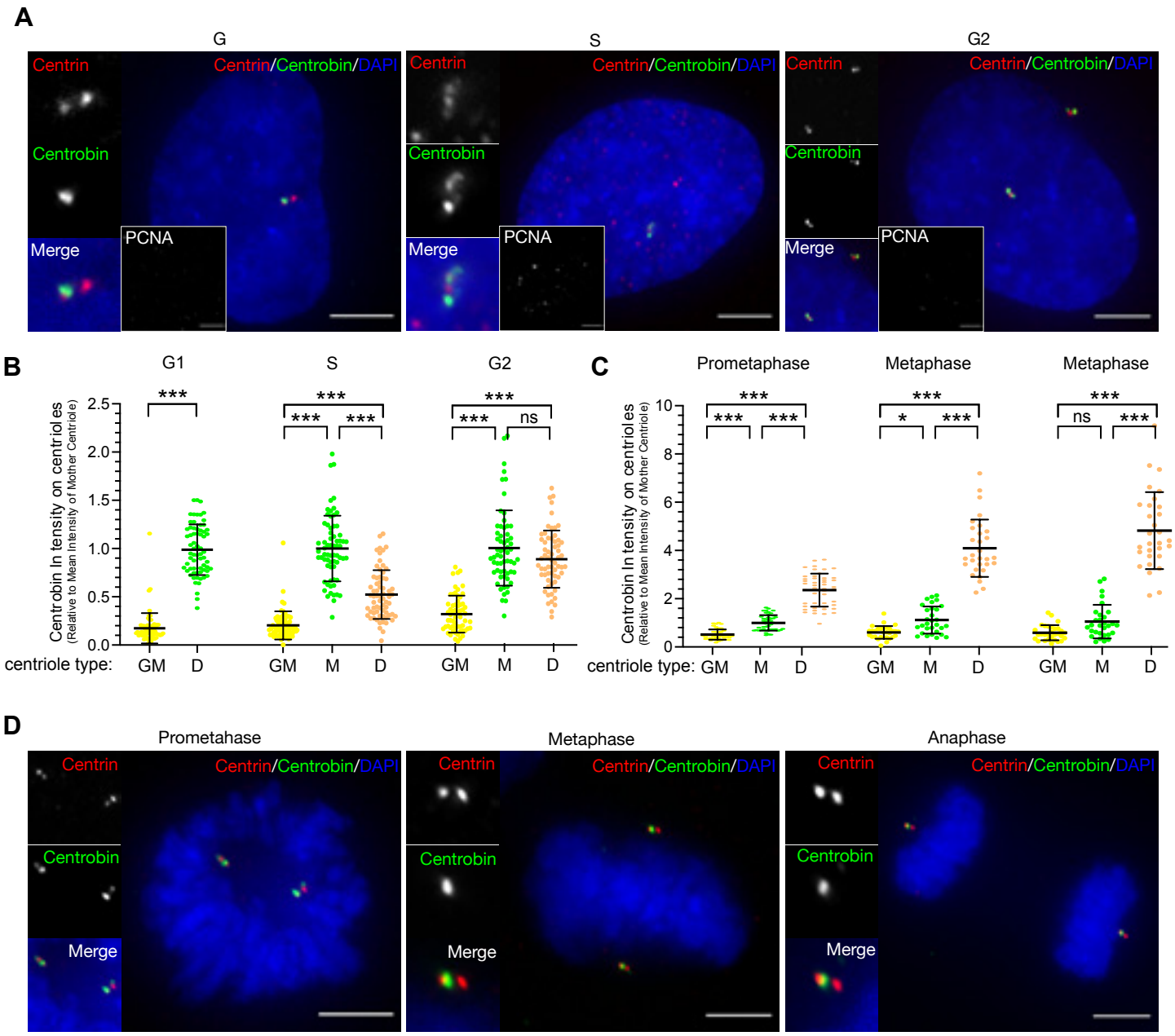

Fig. S1. Centrobin is removed from mother centrioles at the prometaphase/metaphase transition when stained with an alternative centrobin antibody.

(**A**) Immunofluorescence images of hTert-RPE1-eGFP-centrin1 stained with DAPI and antibodies against centrobin and PCNA. (**B**) Quantification of the relative centrobin intensity on individual grandmother (GM), mother (M) and daughter centrioles (D). Values were normalized to the average mother centriole intensity in S (N = 3, n = 67 cells) and G2 (N = 3, n = 62 cells), to the daughter centriole intensity in G1 (N = 3, n = 67 cells). *** $p < 0.001$ in one-way ANOVA, error bars indicate s.e.m. (**C**) Quantification of the relative centrobin intensity on individual grandmother (GM), mother (M) and daughter centrioles (D) in prometaphase (N = 3, n = 47 cells), metaphase (N = 3, n = 30 cells) and anaphase (N = 3, n = 30 cells). Values were normalized to the average mother centriole intensity. * $p < 0.05$, *** $p < 0.001$ in one-way ANOVA, error bars indicate s.e.m. (**D**) Immunofluorescence images of hTert-RPE1-eGFP-centrin1 stained with antibodies against centrobin and DAPI. All scale bars = 5 µm.

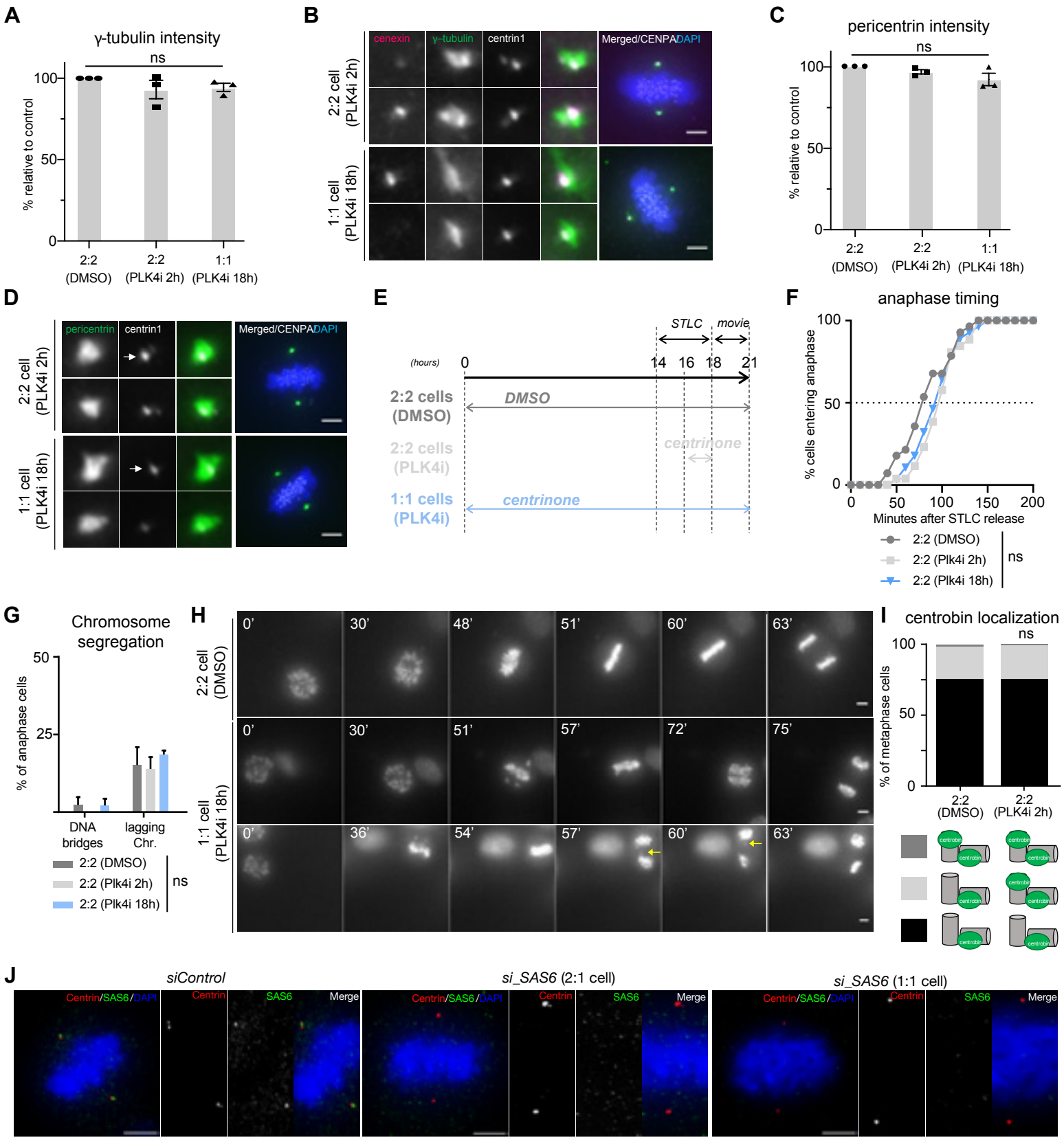

Fig. S2. hTert-RPE1 1:1 cells display normal centrosome function and chromosome segregation. (**A**) Quantification of relative γ-tubulin levels at centrosomes in cells treated with DMSO (N = 3, n = 139 cells) or 250nM centrinone for 2h (N = 3, n = 136 cells) or 18h (N = 3, n = 114 cells); error bars indicate s.e.m. (**B**) Immunofluorescence of metaphase hTert-RPE1 cells treated with centrinone for 2h or 18h stained with DAPI and antibodies against cenexin and γ-tubulin. (**C**) Quantification of relative pericentrin levels at centrosomes in cells treated with DMSO (N = 3, n = 93 cells) or 250nM centrinone for 2h (N = 3, n = 104 cells) or 18h (N = 3, n = 194 cells); error bars indicate s.e.m. (**D**) Immunofluorescence of metaphase hTert-RPE1 cells treated with centrinone for 2h or 18h stained with DAPI and antibodies against cenexin and γ-tubulin. (**E**) Experimental design for the STLC release experiment: cells were treated with DMSO or 250 nM centrinone for 2h or 18h, then blocked in a monopolar conformation with 5μM STLC for 4h, before washing out STLC and observing mitotic progression with SiR-DNA in live cell movies. (**F**) Cumulative frequency of anaphase entry after STLC release (t = 0) in cells treated with DMSO (N = 4, n = 38 cells), 2h with a PLK4 inhibitor (N = 4, n = 26 cells) or 18h with a PLK4 inhibitor (N = 4, n = 28 cells) (**G**) Anaphase outcomes of indicated cells after STLC release in cells treated with DMSO (N = 4, n = 38 cells), 2h with a PLK4 inhibitor (N = 4, n = 18 cells) or 18h with a PLK4 inhibitor (N = 4, n = 28 cells). (**H**) Time-lapse image sequences of hTert-RPE1 cells treated with DMSO or 18h centrinone after STLC release. Yellow arrows indicate lagging chromosomes. Timing is in mins using NEBD as T = 0. (**I**) Quantification of the centrobin localization patterns in hTertRPE1 eGFP-Centrin1/CENPA-eGFP cells treated with DMSO (N = 3, n = 143 cells) or 250nM centrinone for 2h (N = 3, n = 151 cells). (**J**) Immunofluorescence images of hTertRPE1-eGFP-centrin1 cells treated with control or SAS6 siRNA and stained for centrin and DAPI. Note that a 24h SAS6 depletion gave rise to a mix or 2:1 and 1:1 cells. All scale bars = 5 μm.

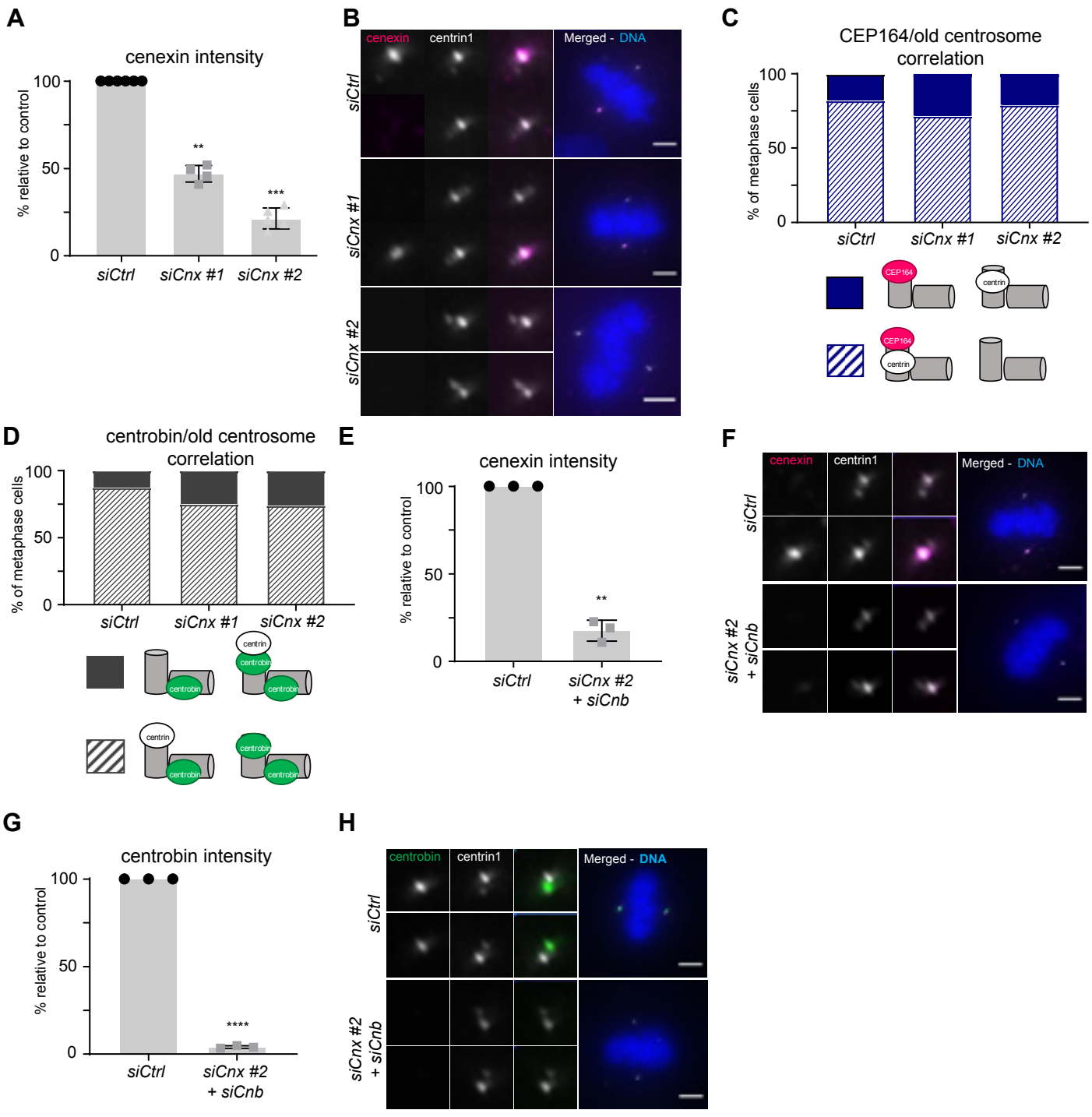

Fig. S3. Cenexin and centrobin depletion efficiencies. (**A**) Quantification of cenexin levels in hTertRPE1 eGFPcentrin1 cells treated with *siCtrl* (N = 4, n = 231 cells), *siCnx #1* (N = 4, n = 153 cells) or *siCnx #2* (N = 4, n = 196 cells) for 48h; **p<0.01 in Anova test; (**B**) Immunofluorescence images of metaphase hTertRPE1 eGFPcentrin1 cells treated with *siCtrl*, *siCnx #1* or *siCnx #2* and stained with DAPI and cenexin antibodies. (**C**) Correlation between the presence of CEP164 at the centriole with the highest eGFP-centrin1 signal in cells treated with *siCtrl* (N = 3, n = 31 cells), *siCnx #1* (N = 3, n = 65 cells) or *siCnx #2* (N = 3, n = 95 cells) for 48h (**D**) Correlation between the absence of centrobin at the centriole with the highest eGFP-centrin1 signal in cells treated with *siCtrl* (N = 3, n = 38 cells), *siCnx #1* (N = 3, n = 63 cells) or *siCnx #2* (N = 3, n = 62 cells) for 48h (**E**) Quantification of cenexin levels in control (N = 3, n = 127 cells) or double depleted cenexin/centrobin (N = 3, n = 116 cells) hTertRPE1 eGFP-centrin1 cells; **p<0.01 in t-test. (**F**) Representative images of cells quantified in (E). (**G**) Quantification of centrobin levels in control (N = 3, n = 144 cells) or double depleted cenexin/centrobin (N = 3, n = 136 cells) hTertRPE1 eGFP-centrin1 cells; ****p<0.0011 in t-test. (**H**) Representative images of cells quantified in (G). All scale bars = 5 µm.

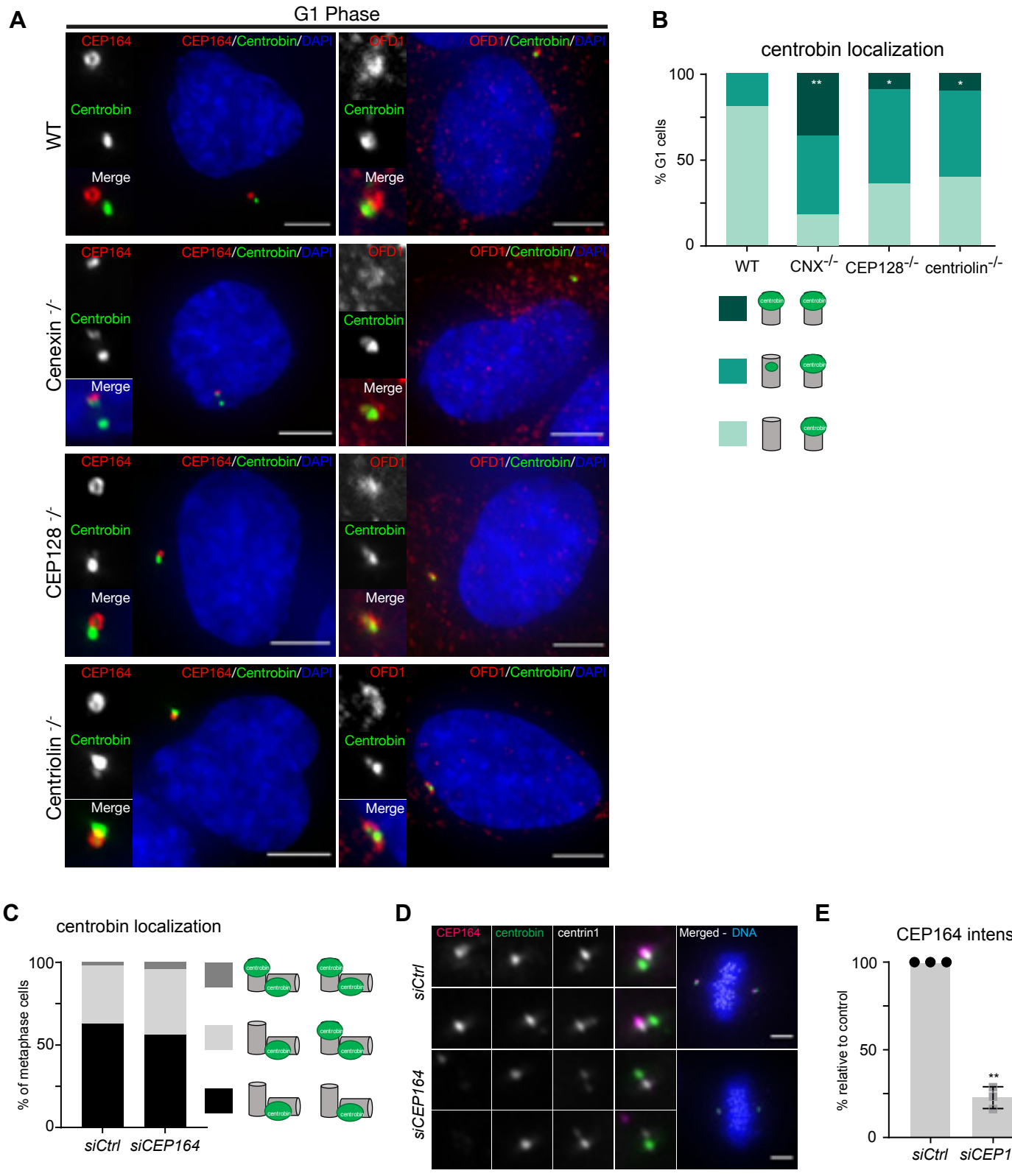

Fig. S4. Effect of subdistal appendage and distal appendage proteins on centrobin localization (A) Immunofluorescence images of WT, cenexin, centriolin or CEP128 knock-out hTert-RPE1 G1 cells stained with DAPI and antibodies against CEP164 and centrobin. (**B**) Quantification of the centrobin localization patterns in parental WT (n = 15 cells), cenexin KO (n = 11 cells), centriolin KO (n = 11 cells) or CEP128 KO (n = 10 cells) hTertRPE1 G1 cells; * $p < 0.05$, ** $p < 0.05$ in Chi-square test. (**C**) Quantification of the centrobin localization patterns in hTertRPE1 eGFP-centrin1/CENPA-GFP cells treated with Ctrl (N = 3, n = 158 cells) or CEP164 (N = 3, n = 91 cells) siRNAs. (**D**) Immunofluorescence